A chemical screen based on an interruption of zebrafish gastrulation identifies the HTR2C inhibitor Pizotifen as a suppressor of EMT-mediated metastasis

Joji Nakayama[1,2,3,4,§], Lora Tan[1], Boon Cher Goh[2], Shu Wang[1, 5], Hideki Makinoshima[3,6] and Zhiyuan Gong[1,§]

[1]Department of Biological Science, National University of Singapore, Singapore
[2]Cancer Science Institute of Singapore, National University of Singapore, Singapore
[3]Tsuruoka Metabolomics Laboratory, National Cancer Center, Tsuruoka, Japan
[4]Shonai Regional Industry Promotion Center, Tsuruoka, Japan.
[5]Institute of Bioengineering and Nanotechnology, Singapore
[6]Division of Translational Research, Exploratory Oncology Research and Clinical Trial Center, National Cancer Center, Kashiwa, Japan.

[§]Corresponding authors:
Joji Nakayama
email: Zmetastasis@gmail.com

Zhiyuan Gong
email: dbsgzy@nus.edu.sg

Keywords: Metastasis, gastrulation, EMT, Phenotyping screening, zebrafish

Total words excluding supplemental figure legends and references section: 5468

Number of figures: 5
Number of tables: 1
Number of supplemental figures: 3
Number of supplemental tables: 2

Abstract

Metastasis is responsible for approximately 90% of cancer-associated mortality but few models exist that allow for rapid and effective screening of anti-metastasis drugs. Current mouse models of metastasis are too expensive and time consuming to use for rapid and high-throughput screening. Therefore, we created a unique screening concept utilizing conserved mechanisms between zebrafish gastrulation and cancer metastasis for identification of potential anti-metastatic drugs. We hypothesized that small chemicals that interrupt zebrafish gastrulation might also suppress metastatic progression of cancer cells and developed a phenotype-based chemical screen to test the hypothesis. The screen used epiboly, the first morphogenetic movement in gastrulation, as a marker and enabled 100 chemicals to be tested in five hours. The screen tested 1280 FDA-approved drugs and identified Pizotifen, an antagonist for serotonin receptor 2C (HTR2C) as an epiboly-interrupting drug. Pharmacologic and genetic inhibition of HTR2C suppressed metastatic progression in a mouse model. Blocking HTR2C with Pizotifen restored epithelial properties to metastatic cells through inhibition of Wnt-signaling. In contrast, HTR2C induced epithelial to mesenchymal transition (EMT) through activation of Wnt-signaling and promoted metastatic dissemination of human cancer cells in a zebrafish xenotransplantation model. Taken together, our concept offers a novel platform for discovery of anti-metastasis drugs.

Introduction

Metastasis, a leading contributor to the morbidity of cancer patients, occurs through multiple steps: invasion, intravasation, extravasation, colonization, and metastatic tumor formation (1-3). The physical translocation of cancer cells is an initial step of metastasis and molecular mechanisms of it involve cell motility, the breakdown of local basement membrane, loss of cell polarity, acquisition of stem cell-like properties, and EMT (4-6). These cell-biological phenomena are also observed during vertebrate gastrulation in that evolutionarily conserved morphogenetic movements of epiboly, internalization, convergence, and extension progress (7). In zebrafish, the first morphogenetic movement, epiboly, is initiated at approximately 4 hours post fertilization (hpf) to move cells from the animal pole to eventually engulf the entire yolk cell by 10 hpf (8, 9). The embryonic cell movements are governed by the molecular mechanisms that are partially shared in metastatic cell dissemination.

At least fifty common genes were shown to be involved in both metastasis and gastrulation progression: Knockdown of these genes in Xenopus or zebrafish induced gastrulation defects; conversely, overexpression of these genes conferred metastatic potential on cancer cells and knockdown of these genes suppressed metastasis (Table S1). This evidence led us to hypothesize that small molecules that interrupt zebrafish gastrulation may suppress metastatic progression of human cancer cells.

Here we report a unique screening concept based on the hypothesis. Pizotifen, an antagonist for HTR2C, was identified from the screen as a “hit” that interrupted zebrafish gastrulation. A mouse model of metastasis confirmed pharmacological and genetic inhibition of HTR2C suppressed metastatic progression. Moreover, HTR2C induced EMT and promoted metastatic dissemination of non-metastatic cancer cells in a zebrafish xenotransplantation model. These results demonstrated that this concept could offer a novel high-throughput platform for discovery of anti-metastasis drugs and can be converted to a chemical genetic screening platform.

Results

Small molecules interrupting epiboly of zebrafish have a potential to suppress metastatic progression of human cancer cells.

Before performing a screening assay, we conducted preliminary experiments to test the hypothesis. First, we examined whether hindering the molecular function of reported genes, whose knockdown induced gastrulation defects in zebrafish, might suppress cell motility and invasion of cancer cells. We chose protein arginine methyltransferase 1 (PRMT1) and cytochrome P450 family 11 (CYP11A1), both of whose knockdown induced gastrulation defects in zebrafish but whose involvement in metastatic progression is unclear (10, 11). Elevated expression of PRMT1 and CYP11A1 were observed in highly metastatic human breast cancer cell lines and knockdown of these genes through RNA interference suppressed the motility and invasion of MDA-MB-231 cells without affecting their viability (Figure S1A-C).

Next, we conducted an inverse examination of whether chemicals which were reported to suppress metastatic dissemination of cancer cells could interrupt epiboly progression of zebrafish embryos. Niclosamide and Vinpocetine are reported to suppress metastatic progression (12, 13) (14, 15). Either Niclosamide or Vinpocetine-treated zebrafish embryos showed complete arrest at very early stages or severe delay in epiboly progression, respectively (Figure S1D).

These results suggest that epiboly could serve as a marker for this screening assay and epiboly-interrupting drugs that are identified through this screening could have the potential to suppress metastatic progression of human cancer cells.

132 FDA-approved drugs induced delayed in epiboly of zebrafish embryos

We screened 1,280 FDA, EMA or other agencies-approved drugs (Prestwick, Inc) in our zebrafish assay. The screening showed that 0.9% (12/1280) of the drugs, including Actimycin A and Tolcapone, induced severe or complete arrest of embryonic cell

103 movement when embryos were treated with 10μM. 5.2% (66/1280) of the drugs, such as
104 Dicumarol, Racecadotril, Pizotifen and S(-) Eticlopride hydrochloride, induced either
105 delayed epiboly or interrupted epiboly of the embryos. 93.3% (1194/1280) of drugs has
106 no effect on epiboly progression of the embryos. 0.6% (8/1280) of drugs induced a toxic
107 lethality. Epiboly progression was affected more severely when embryos were treated
108 with 50μM; 1.7% (22/1280) of the drugs induced severe or complete arrest of it. 8.6%
109 (110/1280) of the drugs induced either delayed epiboly or interrupt epiboly of the
110 embryos. 4.3% (55/1280) of drugs induced a toxic lethality (Figure 1A and 1B, Table S2).
111 Among the epiboly-interrupting drugs, several drugs have already been reported to inhibit
112 metastasis-related molecular mechanisms: Adrenosterone or Zardaverine, which target
113 HSD11β1 or PDE3 and 4, respectively, are reported to inhibit EMT (16, 17);
114 Racecadotril, which targets enkephalinase, is reported to confer metastatic potential on
115 colon cancer cell (18); and Disulfiram, which targets ALDH, is reported to confer stem-
116 like properties on metastatic cancer cells (19). This evidence suggests that epiboly-
117 interrupting drugs have the potential for suppressing metastasis of human cancer cells.
118
119 **Identified drugs suppressed cell motility and invasion of human cancer cells.**
120 It has been reported that zebrafish have orthologues to 86% of 1318 human drug targets
121 (20). However, it was not known whether the epiboly-interrupting drugs could suppress
122 metastatic dissemination of human cancer cells. To test this, we subjected the 78 epiboly-
123 interrupting drugs that showed a suppressor effect on epiboly progression at a 10μM
124 concentration to *in vitro* experiments using a human cancer cell line. The experiments
125 examined whether the drugs could suppress cell motility and invasion of MDA-MB-231
126 cells through a Boyden chamber. Before conducting the experiment, we investigated
127 whether these drugs might effect viability of MDA-MB-231 cells using an MTT assay.
128 Sixteen of the 78 drugs strongly effected cell viability at concentrations less than 1μM
129 and were not used in the cell motility experiments. The remaining 62 drugs were assayed

130 in Boyden chamber motility experiments. Twenty of the 62 drugs inhibited cell motility
131 and invasion of MDA-MB-231 cells without effecting cell viability. Among the 20 drugs,
132 Hexachlorophene and Nitazoxanide were removed since the primary targets of the drugs,
133 D-lactate dehydrogenase and pyruvate ferredoxin oxidoreductase are not expressed in
134 mammalian cells. With the exception of Ipriflavone, whose target is still unclear, the
135 known primary targets of the remaining 17 drugs are reported to be expressed by
136 mammalian cells (Figure 2A and Table 1).
137 We confirmed if highly metastatic human cancer cell lines expressed the genes
138 that code for these targets using Western blotting analyses. Among the genes, serotonin
139 receptor 2C (HTR2C), which is a primary target of Pizotifen, was highly expressed in
140 only metastatic cell lines (Figure 2B). Pizotifen suppressed cell motility and invasion of
141 several highly metastatic human cancer cell lines in a dose-dependent manner (Figure
142 2C). Similarly, Dopamine receptor D2 (DRD2), which is a primary target of S(-)
143 Eticlopride hydrochloride, was highly expressed in only metastatic cell lines, and the drug
144 suppressed cell motility and invasion of these cells in a dose-dependent manner (Figure
145 S2).
146 These results indicate that a number of the epiboly-interrupting drugs also have
147 suppressor effects on cell motility and invasion of highly metastatic human cancer cells.
148
149 **Pizotifen suppressed metastatic dissemination of human cancer cells in a zebrafish**
150 **xenotransplantation model.**
151 While a number of the epiboly-interrupting drugs suppressed cell motility and invasion of
152 human cell lines *in vitro,* it was still unclear whether the drugs could suppress metastatic
153 dissemination of cancer cells in vivo. Therefore, we examined whether the identified
154 drugs could suppress metastatic dissemination of these human cancer cells in a zebrafish
155 xenotransplantation model. Pizotifen was selected to test since HTR2C was overexpressed
156 only in highly metastatic cell lines supporting the hypothesis that it could be a novel target

157 for blocking metastatic dissemination of cancer cells (Figure 2B). Red fluorescent
158 protein-labelled MDA-MB-231 (231R) cells were injected into the duct of Cuvier of *Tg*
159 *(kdrl:eGFP)* zebrafish at 2 dpf and then maintained in the presence of either vehicle or
160 Pizotifen. Twenty-four hours post-injection, the numbers of fish showing metastatic
161 dissemination of 231R cells were measured via fluorescence microscopy. In this model,
162 the dissemination patterns were generally divided into three categories: (i) head
163 dissemination, in which disseminated 231R cells exist in the vessel of the head part; (ii)
164 trunk dissemination, in which the cells were observed in the vessel dilating from the trunk
165 to the tail; (iii) end-tail dissemination, in which the cells were observed in the vessel of
166 the end-tail part (16).

167 Three independent experiments revealed that the frequencies of fish in the drug-
168 treated group showing head, trunk, or end-tail dissemination, significantly decreased to
169 55.3±7.5%, 28.5±5.0% or 43.5±19.1% when compared with those in the vehicle-treated
170 group; 95.8±5.8%, 47.1±7.7% or 82.6±12.7%. Conversely, the frequency of the fish in the
171 drug-treated group not showing any dissemination, significantly increased to 45.4±0.5%
172 when compared with those in the vehicle-treated group; 2.0±2.9% (Figure 2D).

173 Similar effects were observed in another xenograft experiments using an RFP-
174 labelled human pancreatic cancer cell line, MIA-PaCa-2 (MP2R). In the drug treated
175 group, the frequencies of the fish showing head, trunk or end-tail dissemination,
176 significantly decreased to 15.3±6.7%, 6.2±1.3%, or 41.1±1.5%; conversely, the frequency
177 of the fish not showing any dissemination significantly increased to 46.3±8.9% when
178 compared with those in the vehicle-treated group; 74.5±11.1%, 18.9±14.9%, 77.0±9.0%,
179 or 17.2±0.7% (Figure S3).

180 To eliminate the possibility that the metastasis suppressing effects of Pizotifen
181 might result from off-target effects of the drug, we conducted validation experiments to
182 determine whether knockdown of HTR2C would show the same effects. Sub-clones of
183 231R cells that expressed shRNA targeting either LacZ or HTR2C were injected into the

184 fish at 2 dpf and the fish were maintained in the absence of drug. In the fish that were
185 inoculated with shHTR2C 231R cells, the frequencies of the fish showing head, trunk,
186 and end-tail dissemination, significantly decreased to 6.7±4.9%, 6.7±0.7%, or
187 20.0±16.5%; conversely, the frequency of the fish not showing any dissemination,
188 significantly increased to 80.0±4.4% when compared with those that were inoculated with
189 shLacZ 231R cells; 80.0±27.1%, 20.0±4.5%, 90.0± 7.7%, or 0% (Figure 2E).
190 These results indicate that pharmacological and genetic inhibition of HTR2C
191 suppressed metastatic dissemination of human cancer cells in vivo.
192
193 **Pizotifen suppressed metastasis progression of a mouse model of metastasis.**
194 We examined the metastasis-suppressor effect of Pizotifen in a mouse model of
195 metastasis (21). Luciferase-expressing 4T1 murine mammary carcinoma cells were
196 inoculated into the mammary fat pads (MFP) of female BALB/c mice. On day two
197 post inoculation, the mice were randomly assigned to two groups and one group
198 received once daily intraperitoneal injections of 10mg/kg Pizotifen while the other
199 group received a vehicle injection. Bioluminescence imaging and tumor measurement
200 revealed that the sizes of the primary tumors in Pizotifen-treated mice were equal to
201 those in the vehicle-treated mice at the time of resection on day 10 post inoculation.
202 Immunofluorescent staining also demonstrated that the percentage of Ki67 positive
203 cells in the resected primary tumors of Pizotifen-treated mice were the same as those
204 of vehicle-treated mice (Figure 3A-C), additionally, both groups showed less than 1%
205 cleaved caspase 3 positive cells (data not shown). Therefore, no anti-tumor effect of
206 Pizotifen was observed on the primary tumor. After 70 days from inoculation,
207 bioluminescence imaging detected light emitted in the lungs, livers and lymph nodes
208 of vehicle-treated mice but not those of Pizotifen-treated mice (Figure 3C). Vehicle-
209 treated mice formed 5 to 50 metastatic nodules per lung in all 10 mice analyzed;
210 conversely, Pizotifen-treated mice (n=10) formed 0 to 5 nodules per lung in all 10

211 mice analyzed (Figure 3D). Histological analyses confirmed that metastatic lesions in
212 the lungs were detected in all vehicle-treated mice; conversely, they were detected in
213 only 2 of 10 Pizotifen-treated mice and the rest of the mice showed metastatic colony
214 formations around the bronchiole of the lung. In addition, 4 of 10 vehicle-treated mice
215 exhibited metastasis in the liver and the rest showed metastatic colony formation
216 around the portal tract of the liver. In contrast, none of 10 Pizotifen-treated mice
217 showed liver metastases and only half of the 10 mice showed metastatic colony
218 formation around the portal tract (Figure 3E). These results indicate that Pizotifen can
219 suppress metastasis progression without affecting primary tumor growth.
220 To eliminate the possibility that the metastasis suppressing effects of Pizotifen
221 might result from off-target effects, we conducted validation experiments to determine
222 whether knockdown of HTR2C would show the same effects. The basic experimental
223 process followed the experimental design described above except that sub-clones of
224 4T1 cells that expressed shRNA targeting either LacZ or HTR2C were injected into
225 the MFP of female BALB/c mice and the mice were maintained without drug.
226 Histological analyses revealed that all of the mice (n=5) that were inoculated with 4T1
227 cells expressing shRNA targeting LacZ showed metastases in the lungs. The mean
228 number of metastatic lesions in a lung was 26.4±7.8. In contrast, only one of the mice
229 (n=5) were inoculated with 4T1 cells expressing shRNA targeting HTR2C showed
230 metastases in the lungs and the rest of the mice showed metastatic colony formation
231 around the bronchiole of the lung. The mean number of metastatic lesions in the lung
232 significantly decreased to 10% of those of mice that were inoculated with 4T1 cells
233 expressing shRNA targeting LacZ (Figure 3F-H).
234 Taken together, pharmacological and genetic inhibition of HTR2C showed an
235 anti-metastatic effect in the 4T1 model system.
236

237 **HTR2C promoted EMT-mediated metastatic dissemination of human cancer cells**

238 Although pharmacological and genetic inhibition of HTR2C inhibited metastasis
239 progression, a role for HTR2C on metastatic progression has not been reported.
240 Therefore, we examined whether HTR2C could confer metastatic properties on poorly
241 metastatic cells.

242 Firstly, we established a stable sub-clone of MCF7 human breast cancer cells
243 expressing either vector control or HTR2C. Vector control expressing MCF7 cells
244 maintained highly organized cell-cell adhesion and cell polarity; however, HTR2C-
245 expressing MCF7 cells led to loss of cell-cell contact and cell scattering. The cobblestone-
246 like appearance of these cells was replaced by a spindle-like, fibroblastic morphology.
247 Western blotting and immunofluorescence (IF) analyses revealed that HTR2C-expressing
248 MCF7 cells showed loss of E-cadherin and EpCAM, and elevated expressions of N-
249 cadherin, vimentin and an EMT-inducible transcriptional factor Zeb1. Similar effects
250 were validated through another experiment using an immortal keratinocyte cell line,
251 HaCaT cells, in that HTR2C-expressing HaCaT cells also showed loss of cell-cell contact
252 and cell scattering with loss of epithelial markers and gain of mesenchymal markers
253 (Figure 4A-C). Therefore, both the morphological and molecular changes in the HTR2C-
254 expressing MCF7 and HaCaT cells demonstrated that these cells had undergone an EMT.

255 Next, we examined whether HTR2C-driven EMT could promote metastatic
256 dissemination of human cancer cells. Boyden chamber assay revealed that HTR2C
257 expressing MCF7 cells showed an increased cell motility and invasion compared with
258 vector control-expressing MCF7 cells in vitro (Figure 4D). Moreover, we conducted in
259 vivo examination of whether HTR2C expression could promote metastatic dissemination
260 of human cancer cells in a zebrafish xenotransplantation model. Red fluorescence protein-
261 labelled MCF7 cells expressing either vector control or HTR2C were injected into the
262 duct of Cuvier of *Tg* (*kdrl:eGFP*) zebrafish at 2 dpf. Twenty-four hours post injection, the
263 frequencies of the fish showing metastatic dissemination of the inoculated cells were

264 measured using fluorescence microscopy. In the fish that were inoculated with HTR2C
265 expressing MCF7 cells, the frequencies of the fish showing head, trunk, and end-tail
266 dissemination significantly increased to 96.7±4.7%, 68.8±6.4%, or 89.5±3.4%;
267 conversely, the frequency of the fish not showing any dissemination decreased to 0%
268 when compared with those in the fish that were inoculated with vector control expressing
269 MCF7 cells; 33.1±18.5%, 0%, 56.9± 4.4%, or 43% (Figure 4E).
270 These results indicated that HTR2C promoted metastatic dissemination of cancer
271 cells though induction of EMT, and suggest that the screen can easily be converted to a
272 chemical genetic screening platform.
273
274 **Pizotifen induced mesenchymal to epithelial transition through inhibition of Wnt-**
275 **signaling.**
276 Finally, we elucidated the mechanism of action of how Pizotifen suppressed metastasis,
277 especially metastatic dissemination of cancer cells. Our results showed that HTR2C
278 induced EMT and that pharmacological and genetic inhibition of HTR2C suppressed
279 metastatic dissemination of MDA-MB-231 cells that had already transitioned to
280 mesenchymal-like traits via EMT. Therefore, we speculated that blocking HTR2C with
281 Pizotifen might inhibit the molecular mechanisms which follow EMT induction. We
282 firstly investigated the expressions of epithelial and mesenchymal markers in Pizotifen-
283 treated MDA-MB-231 cells since the activation of an EMT program needs to be transient
284 and reversible, and transition from a fully mesenchymal phenotype to a epithelial-
285 mesenchymal hybrid state or a fully epithelial phenotype is associated with malignant
286 phenotypes (22). IF and FACS analyses revealed 20% of Pizotifen-treated MDA-MB-231
287 cells restored E-cadherin expression. Also, western blotting analysis demonstrated that
288 4T1 primary tumors from Pizotifen-treated mice has elevated E-cadherin expression
289 compared with tumors from vehicle-treated mice (Figure 5A-C). However, mesenchymal
290 markers did not change between vehicle and Pizotifen-treated MDA-MB-231 cells (data

291 not shown). We further analyzed E-cadherin positive (E-cad$^+$) cells in Pizotifen-treated
292 MDA-MB-231 cells. The E-cad$^+$ cells showed elevated expressions of epithelial markers
293 KRT14 and KRT19; and decreased expression of mesenchymal makers vimentin, MMP1,
294 MMP3, and S100A4. Recent research reports that an EMT program needs to be transient
295 and reversible and that a mesenchymal phenotype in cancer cells is achieved by
296 constitutive ectopic expression of Zeb1. In accordance with the research, the E-cad$^+$ cells
297 and 4T1 primary tumors from Pizotifen-treated mice had decreased Zeb1 expression
298 compared with vehicle-treated cells and tumors from vehicle-treated mice (Figure 5D). In
299 contrast, HTR2C-expressing MCF7 and HuMEC cells expressed Zeb1 but not vehicle
300 control MCF7 and HuMEC cells (Figure 4C). These results indicate that HTR2C-
301 mediated signaling induced EMT through up-regulation of Zeb1 and blocking HTR2C
302 with Pizotifen induced mesenchymal to epithelial transition through downregulation of
303 Zeb1.
304 We further investigated the mechanism of action of how blocking HTR2C with
305 Pizotifen induced down-regulation of Zeb1. In embryogenesis, serotonin-mediated
306 signaling is required for Wnt-dependent specification of the superficial mesoderm during
307 gastrulation (23). In cancer cells, overexpression of HTR1D is associated with Wnt-
308 signaling which enables induction of EMT (24, 25). This evidence led to a hypothesis that
309 HTR2C-mediated signaling might turn on transcriptional activity of β-catenin and that
310 might induce up-regulation of EMT-TFs. IF analyses revealed β-catenin was accumulated
311 in the nucleus of HTR2C-expressing MCF7 cells but it was located in the cytoplasm of
312 vector control-expressing cells (Figure 5E). Nuclear accumulation of β-catenin in
313 HTR2C-expressing MCF7 cells was confirmed by western blot (Figure 5F). In contrast,
314 Pizotifen-treated MDA-MB-231 cells showed β-catenin located in the cytoplasm of the
315 cells. Vehicle-treated cells showed β-catenin accumulated in the nucleus of the cells.
316 (Figure 5G), and western blotting analysis confirmed that it was located in the cytoplasm
317 of Pizotifen-treated MDA-MB-231 cells (Figure 5H). Furthermore,

318 immunohistochemistry and western blotting analyses showed that β-catenin accumulated
319 in the nucleus, and phospho-GSKβ and Zeb1 expression were decreased in 4T1 primary
320 tumors from Pizotifen-treated mice compared with vehicle-treated mice (Figure 5C).
321 These results indicated that HTR2C would regulate transcriptional activity of β-catenin
322 and Pizotifen could inhibit it.
323 Taken together, we conclude that blocking HTR2C with Pizotifen restored
324 epithelial properties to metastatic cells (MDA-MB-231 and 4T1 cells) through a decrease
325 of transcriptional activity of β-catenin and that suppressed metastatic progression of the
326 cells.
327

328 **Figures and figure legends**

329 **Figure 1**

330

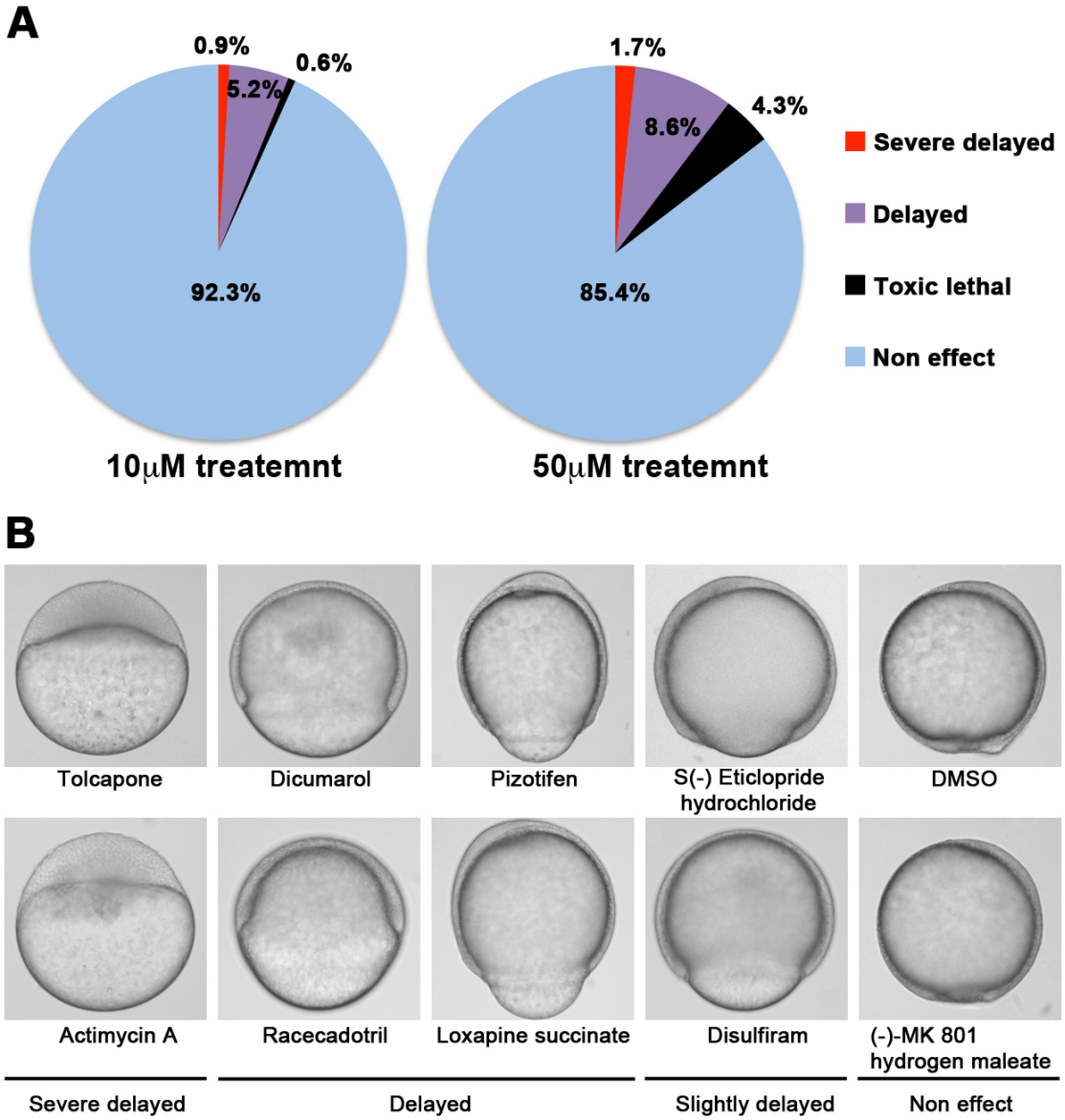

331

332

333 **Figure 1. A chemical screen for identification of epiboly-interrupting drugs.**

334 (A) Cumulative results of the chemical screen in which each drug was used at either

335 10μM (left) or 50μM (right) concentrations. 1,280 FDA, EMA or other agencies-

336 approved drugs were subjected to this screening. Positive "hit" drugs were those that

337 interrupted epiboly progression. (B) Representative samples of the embryos that were

338 treated with indicated drugs.

339 **Figure 2**

340

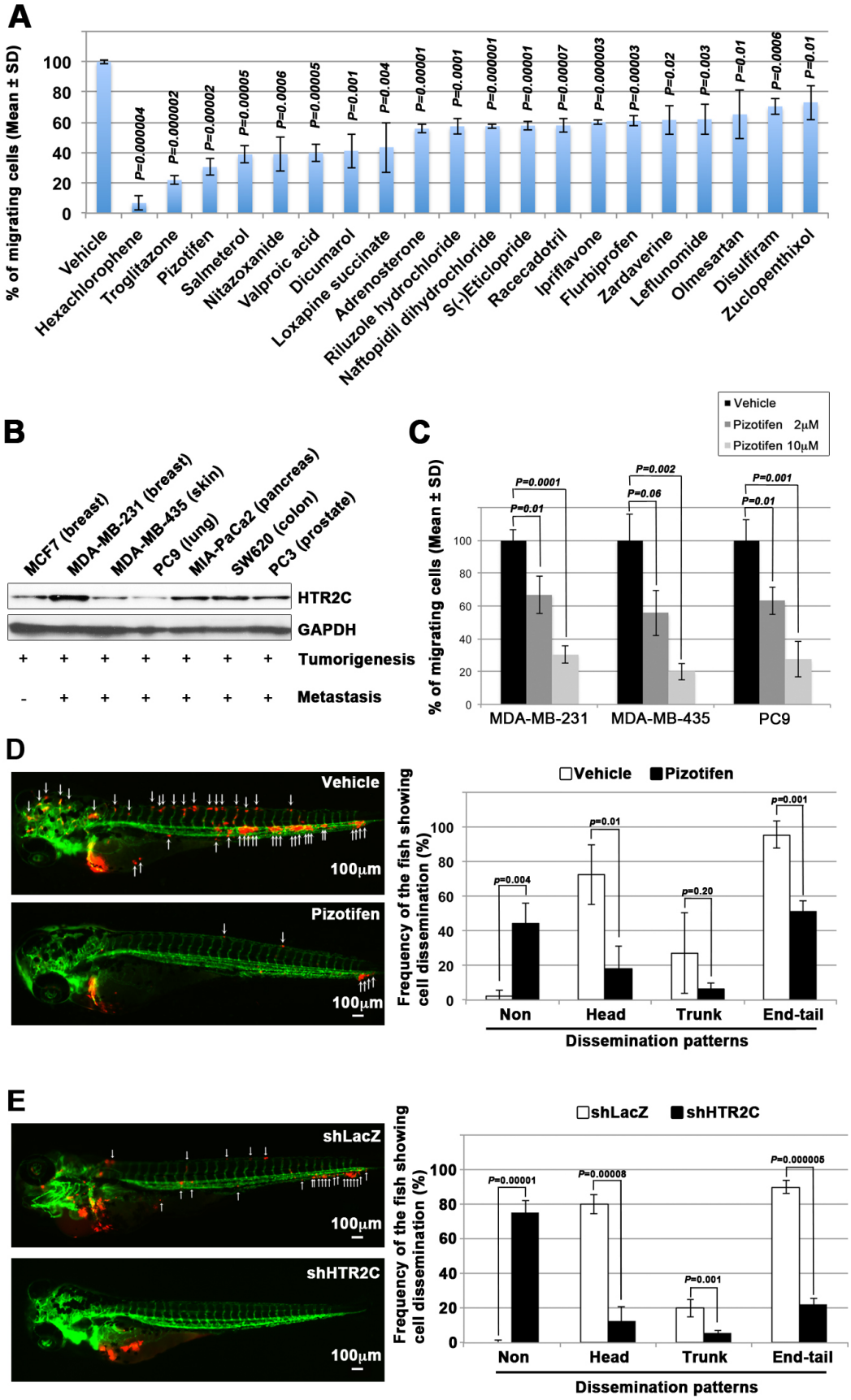

341

342 **Figure 2. Pizotifen, one of epiboly-interrupting drugs suppressed metastatic**

343 **dissemination of human cancer cells lines in vivo and vitro.**

344 (A) Effect of the epiboly-interrupting drugs on cell motility and invasion of MBA-MB-
345 231 cells. MBA-MB-231 cells were treated with vehicle or each of the epiboly-
346 interrupting drugs and then subjected to Boyden chamber assays. Fetal bovine serum
347 (1%v/v) was used as the chemoattractant in both assays. Each experiment was performed
348 at least twice. (B) Western blot analysis of HTR2C levels (top) in a non-metastatic human
349 cancer cell line, MCF7 (breast) and highly metastatic human cancer cell lines, MDA-MB-
350 231 (breast), MDA-MB-435 (melanoma), MIA-PaCa2 (pancreas), PC3 (prostate) and
351 SW620 (colon); GAPDH loading control is shown (bottom). (C) Effect of pizotifen on
352 cell motility and invasion of MBA-MB-231, MDA-MB-435 and PC9 cells. Either vehicle
353 or pizotifen treated the cells were subjected to Boyden chamber assays. Fetal bovine
354 serum (1%v/v) was used as the chemoattractant in both assays. Each experiment was
355 performed at least twice. (D) and (E) Representative images of dissemination of 231R,
356 shLacZ 231R or shHTR2C 231R cells in zebrafish xenotransplantation model. The fish
357 larvae that were inoculated with 231R cells, were treated with either vehicle (top left) or
358 the drug (lower left) (D). The fish larvae that were inoculated with either shLacZ 231R or
359 shHTR2C 231R cells (lower left) (E). White arrows head indicate disseminated 231R
360 cells. The images were shown in 4x magnification. Scale bar, 100µm. The mean
361 frequencies of the fish showing head, trunk, or end-tail dissemination were counted
362 (graph on right). Each value is indicated as the mean ± SEM of two independent
363 experiments. Statistical analysis was determined by Student's t test. See also Figure S2
364 and S3.
365

366 **Figure 3**

367

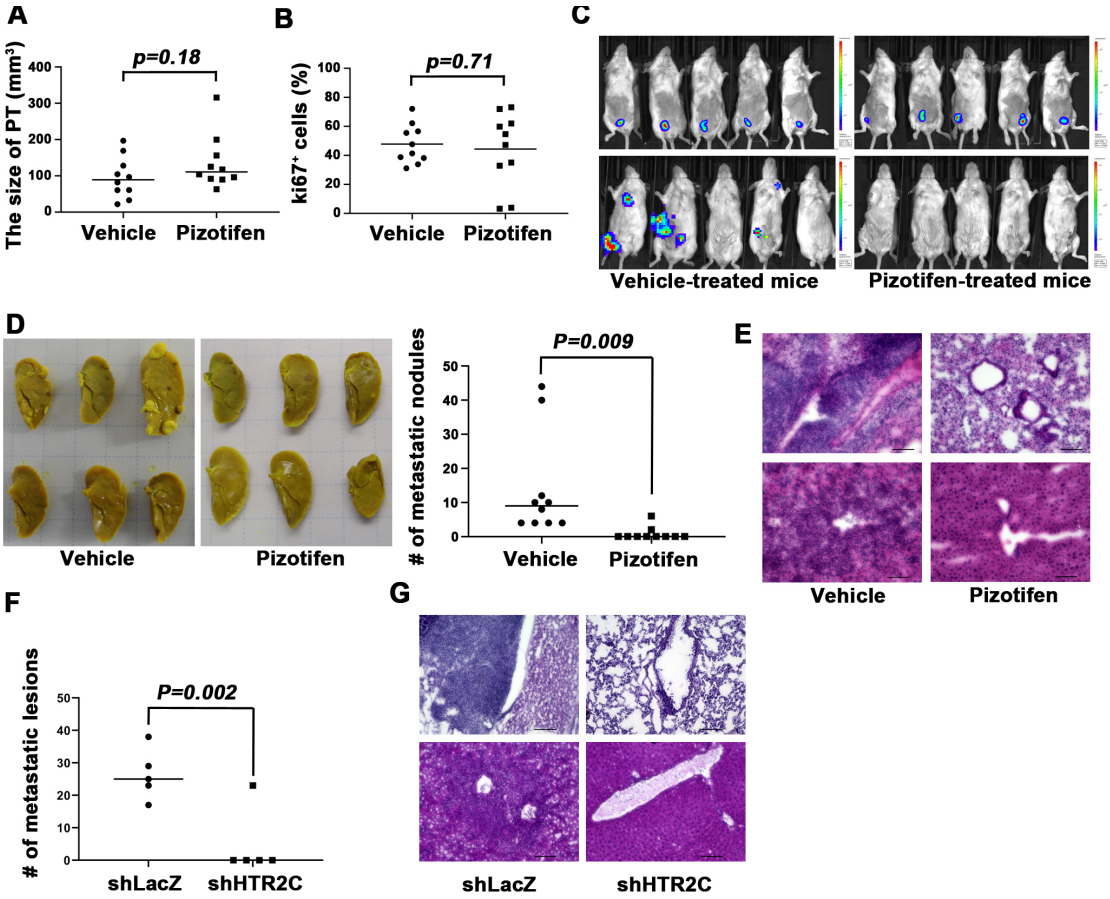

368

369

370 **Figure 3. Pizotifen suppressed metastatic progression in a mouse model of**

371 **metastasis.**

372 (A) Mean volumes (n=10 per group) of 4T1 primary tumors formed in the mammary fat

373 pad of either vehicle or Pizotifen-treated mice at day 10 post injection. (B) Ki67

374 expression level in 4T1 primary tumors formed in the mammary fat pad of either vehicle

375 or Pizotifen-treated mice at day 10 post injection. The mean expression levels of Ki67

376 (n=10 mice per group) were determined and were calculated as the mean ration of Ki67

377 positive cells to DAPI area. (C) Representative images of primary tumors on day 10 post

378 injection (top panels) and metastatic burden on day 70 post injection (bottom panels)

379 taken using an IVIS Imaging System. (D) Representative images of the lungs from either

380 vehicle (top) or Pizotifen-treated mice (bottom) at 70 days past tumor inoculation.

381 Number of metastatic nodules in the lung of either vehicle or Pizotifen-treated mice
382 (right). (E) Representative H&E staining of the lung (top) and liver (bottom) from either
383 vehicle or Pizotifen-treated mice. (F) The mean number of metastatic lesions in step
384 sections of the lungs from the mice that were inoculated with 4T1-12B cells expressing
385 shRNA targeting for either LacZ or HTR2C. (G) Representative H&E staining of the lung
386 and liver from the mice that were inoculated with 4T1-12B cells expressing shRNA
387 targeting for either LacZ or HTR2C. Each value is indicated as the mean ± SEM.
388 Statistical analysis was determined by Student's *t* test.
389

390 **Figure 4**

391

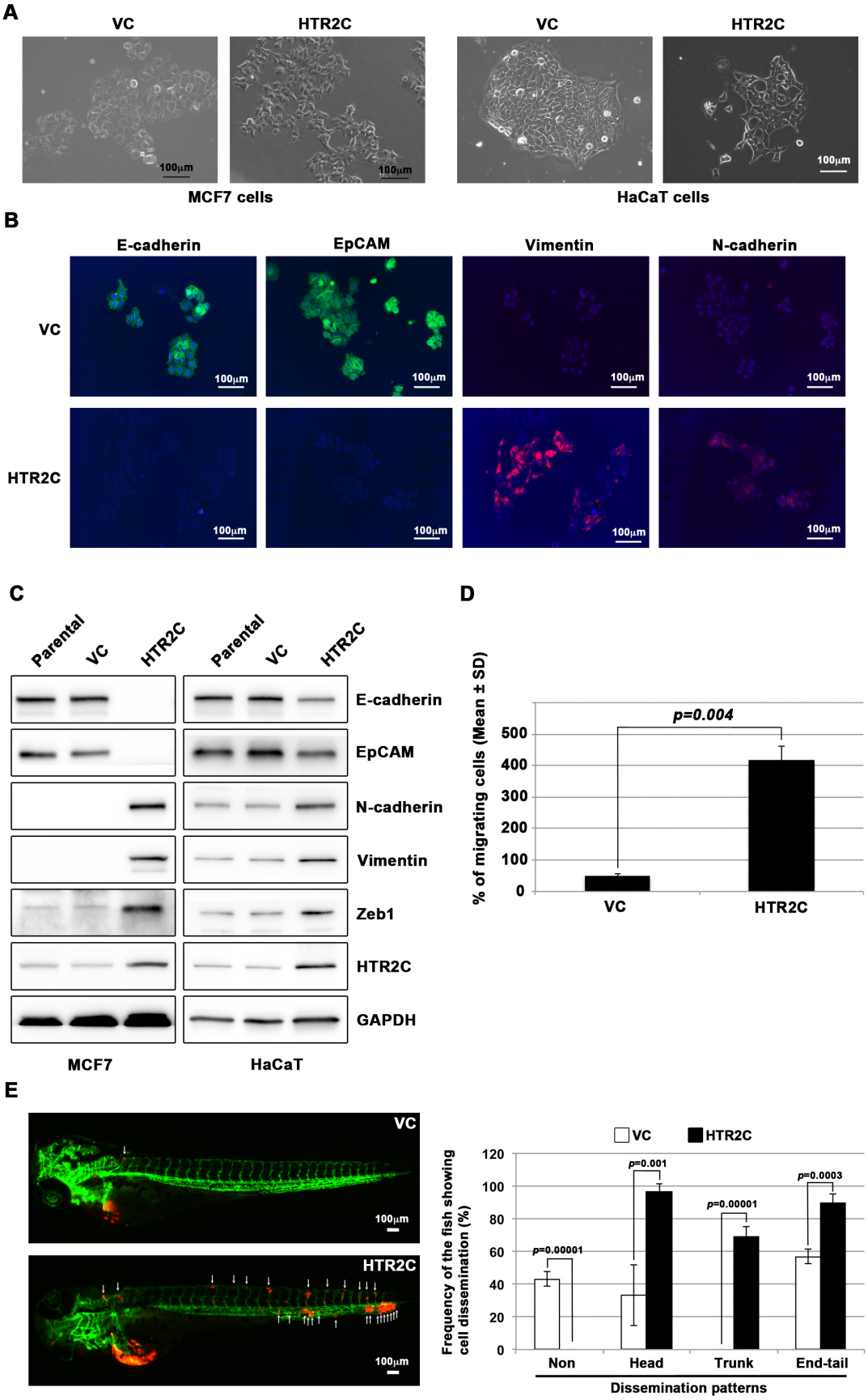

392

393 **Figure 4. HTR2C induced EMT-mediated metastatic dissemination of human cancer**
394 **cells.**
395 (A) The morphologies of the MCF7 and HaCaT cells expressing either the control vector
396 or HTR2C were revealed by phase contrast microscopy. (B) Immunofluorescence staining
397 of E-cadherin, EpCAM, Vimentin, and N-cadherin expressions in the MCF7 cells from
398 Figure 4A. (C) Expression of E-cadherin, EpCAM, Vimentin, N-cadherin, and HTR2C
399 was examined by western-blotting in the MCF7 and HaCaT cells; GAPDH loading
400 control is shown (bottom). (D) Effect of HTR2C on cell motility and invasion of MCF7
401 cells. MCF7 cells were subjected to Boyden chamber assays. Fetal bovine serum (1%v/v)
402 was used as the chemoattractant in both assays. Each experiment was performed at least
403 twice. (E) Representative images of dissemination patterns of MCF7 cells expressing
404 either the control vector (top left) or HTR2C (lower left) in a zebrafish
405 xenotransplantation model. White arrows head indicate disseminated MCF7 cells. The
406 mean frequencies of the fish showing head, trunk, or end-tail dissemination tabulated
407 (right). Each value is indicated as the mean ± SEM of two independent experiments.
408 Statistical analysis was determined by Student's *t* test.
409

410 **Figure 5**

411

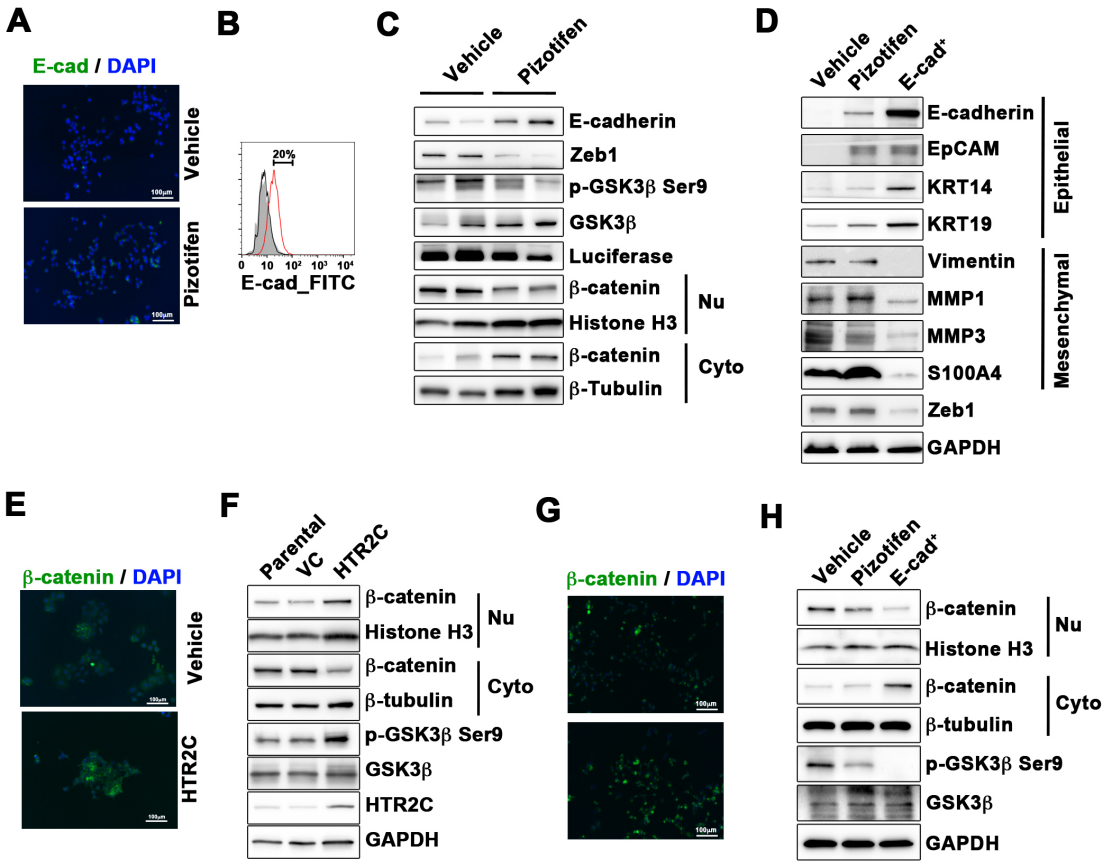

412

413 **Figure 5. Pizotifen restored mesenchymal-like traits of MDA-MB-231 cells into**

414 **epithelial traits through blocking nuclear accumulation of β-catenin.**

415 (A) IF staining of E-cadherin in either vehicle or Pizotifen-treated MDA-MB-231 cells.

416 (B) Surface expression of E-cadherin in either vehicle (black) or Pizotifen (red)-treated

417 MDA-MB-231 cells by FACS analysis. Non-stained controls are shown in gray. (C)

418 Protein expressions levels of E-cadherin, Zeb1, and β-catenin in the cytoplasm and

419 nucleus of 4T1 primary tumors from either vehicle or Pizotifen-treated mice are shown;

420 Luciferase, Histone H3, and β-tubulin are used as loading control for whole cell, nuclear

421 or cytoplasmic lysate, respectively. (D) Protein expression levels of epithelial and

422 mesenchymal markers and Zeb1 in either vehicle or Pizotifen-treated MDA-MB-231 cells

423 or E-cadherin positive (E-cad^{+}) cells in Pizotifen-treated MDA-MB-231 cells are shown.

424 (E) Immunofluorescence staining of β-catenin in the MCF7 cells expressing either vector

425 control or HTR2C. (F) Expressions of β-catenin in the cytoplasm and nucleus of MCF7

426 cells. (G) IF staining of β-catenin in either vehicle or Pizotifen-treated MDA-MB-231

427 cells. (H) Expressions of β-catenin in the cytoplasm and nucleus of MDA-MB-231 cells

428 and the E-cad^{+} cells.

429

430 **Table 1. Primary targets of the identified drugs**

431

The identified drugs	Primary targets of the identified drugs
Hexachlorophene	D-lactate dehydrogenase (D-LDH), not expressed in mammalian cells
Troglitazone	Agonist for Peroxisome proliferator-activated receptor α and γ (PPARα and γ)
Pizotifen malate	5-hydroxytryptamine receptor 2C (HTR2C)
Salmeterol	Adrenergic receptor beta 2 (ADRB2)
Nitazoxanide	Pyruvate ferredoxin oxidoreductase (PFOR), not expressed in mammalian cells
Valproic acid	Histone deacetylases (HDACs)
Dicumarol	NAD(P)H dehydrogenase quinone 1 (NQO1)
Loxapine succinate	Dopamine receptor D2 and D4 (DRD2 and DRD4)
Adrenosterone	Hydroxysteroid (11-beta) dehydrogenase 1 (HSD11β1)
Riluzole hydrochloride	Glutamate R and Voltage-dependent Na+ channel
Naftopidil dihydrochloride	5-hydroxytryptamine receptor 1A (HTR1A) and α1-adrenergic receptor (AR)
S(-)Eticlopride hydrochloride	Dopamine receptor D2 (DRD2)
Racecadotril	Membrane metallo-endopeptidase (MME)
Ipriflavone	Unknow
Flurbiprofen	Cyclooxygenase 1 and 2 (Cox1 and 2)
Zardaverine	Phosphodiesterase III/IV (PDE3/4)
Leflunomide	Dihydroorotate dehydrogenase (DHODH)
Olmesartan	Angiotensin II receptor alpha
Disulfiram	Aldehyde dehydrogenase (ALDH) Dopamine β-hydroxylase (DBH)
Zuclopenthixol dihydrochloride	Dopamine receptors D1 and D2 (DRD1 and 2)

432

433

434

435

436

437 **Discussion**

438 Reducing or eliminating mortality associated with metastatic disease is a key goal of
439 medical oncology, but few models exist that allow for rapid, effective screening of novel
440 compounds that target the metastatic dissemination of cancer cells. Based on accumulated
441 evidence that at least fifty genes play an essential role in governing both metastasis and
442 gastrulation progression (Table 1S), we hypothesized that small molecule inhibitors that
443 interrupt gastrulation of zebrafish embryos might suppress metastatic progression of
444 human cancer cells. We created a unique screening concept utilizing gastrulation of
445 zebrafish embryos to test the hypothesis. Our results clearly confirmed our hypothesis:
446 25.6% (20/76 drugs) of epiboly-interrupting drugs could also suppress cell motility and
447 invasion of highly metastatic human cell lines in vitro. In particular, Pizotifen which is an
448 antagonist for serotonin receptor 2C and one of the epiboly-interrupting drugs, could
449 suppress metastasis in a mouse model (Figure 3A-E). Thus, this screen could offer a novel
450 platform for discovery of anti-metastasis drugs.

451 There are at least two advantages to the screen described herein. One is that the
452 screen can easily be converted to a chemical genetic screening platform. Indeed, we have
453 provided the first evidence that HTR2C, which is a primary target of Pizotifen, induced
454 EMT and promoted metastatic dissemination of cancer cells (Figure 4A-E). In this
455 research, 1,280 FDA approval drugs were screened, this is less than a few percent of all of
456 druggable targets (approximately 100 targets) in the human proteome in the body. If
457 chemical genetic screening using specific inhibitor libraries were conducted, more genes
458 that contribute to metastasis and gastrulation could be identified. The second advantage is
459 that the screen enables one researcher to test 100 drugs in 5 hours with using optical
460 microscopy, drugs, and zebrafish embryos. That indicates this screen is not only highly
461 efficient, low-cost, and low-labor but also enables researchers who do not have high
462 throughput screening instruments to conduct drug screening for anti-metastasis drugs.
463

464 **Acknowledgments**

465 We sincerely appreciate Dr. Joshua Collins (NIH/NIDCR) and Dr. Diane Palmieri
466 (NIH/NCI) for helping this research. We thank Dr. Herrick (Albany medical collage) for
467 providing pCMV-h5TH2C-VSV with us. This study was funded by grants from National
468 Medical Research Council of Singapore (R-154000547511) and Ministry of Education of
469 Singapore (R-154000A23112) to Z.G.

470

471 **Author Contributions**

472 Design research; J.N. Conducting experiments; J.N. and L.T. Analyzing data: J.N.
473 Writing the paper; J.N. and Z.G. Funding Acquisition; Z.G, S.W. B.C.G., H.M. and
474 Supervision; Z.G.

475

476 **Declaration of Interests**

477 J.N., L.T., B.C.G., S.W., H.M. and G.Z. declare no conflict of interest.

478

479 **Materials and Methods**

480 **Zebrafish embryo screening**

481 Each drug was added to a well of a 24-well plate containing approximately 20 zebrafish
482 embryos per well in either 10 μM or 50 μM final concentration when the embryos reached
483 the sphere stage. Chemical treatment was initiated at 4 hours post-fertilization (hpf) and
484 approximately 20 embryos were treated with two different concentrations for each
485 compound tested. The treatment was ended at 9 hpf when vehicle (DMSO) treated
486 embryos as control reach 80-90% completion of the epiboly stage. The compounds which
487 induced delay (<50% epiboly) in epiboly were selected as hit compounds for in vitro
488 testing using highly metastatic human cancer cell lines. The study protocol was approved
489 by the Institutional Animal Care and Use Committee of the National University of
490 Singapore (protocol number: R16-1068).

491

492 **Reagents**

493 FDA, EMA and other agencies approved chemical libraries was purchased from
494 Prestwick Chemical (Illkirch, France). Pizotifen and S(-) Eticlopride hydrochloride were
495 purchased from Sigma-Aldrich (St. Louis, MO).

496

497 **Cell culture and cell viability assay**

498 MCF7, MDA-MB-231, MDA-MB-435, MIA-PaCa2, PC3, SW620, PC9 and HaCaT cells
499 were obtained from American Type Culture Collection (ATCC, Manassas, VA).
500 Luciferase-expressing 4T1 (4T1-12B) cells were provided from Dr. Gary Sahagian
501 (Tufts University, Boston, MA). All culture methods followed the supplier's instruction.
502 Cell viability assay was performed as previously described (16).

503

504 **Plasmid**

505 A DNA fragment coding for HTR2C was amplified by PCR with primers containing
506 restriction enzyme recognition sequences. The HTR2C coding fragment was amplified
507 from hsp70l:mCherry-T2A-CreERT2 plasmid (17).

508

509 **Immunoblotting**

510 Western blotting was performed as described previously (16). Anti-PRMT1, anti-
511 CYP11A1, anti-E-cadherin, anti-EpCAM, anti-Vimentin, anti-N-cadherin, anti-Zeb1,
512 anti-Histone H_3, anti-α-tubulin and anti-GAPDH antibodies were purchased from Cell
513 signaling Technology. Anti-HTR2C and anti-DRD2 antibodies were purchased form
514 Abcam. Anti-phospho-GSK3β (Ser9), anti-GSK3β, Anti-KRT14, anti-KRT19, anti-
515 MMP1, anti-MMP2, anti-S100A4, anti-Luciferase, and anti-β-catenin antibodies were
516 purchased from Santa Cruz.

517

518 **Flow cytometry**

519 Cells were stained with FITC-conjugated E-cadherin antibody (Biolegend, San Diego,
520 CA). Flow cytometry was performed as described (26) and analyzed with FlowJo
521 software (TreeStar, Ashland, OR).

522

523 **shRNA mediated gene knockdown**

524 The short hairpin RNA (shRNA)-expressing lentivirus vectors were
525 constructed using pLVX-shRNA1 vector (Clontech). PRMT1-shRNA_#3–targeting
526 sequence is GTGTTCCAGTATCTCTGATTA; PRMT1-shRNA_#4–targeting sequence
527 is TTGACTCCTACGCACACTTTG. CYP11A1-shRNA_#4–targeting sequence is
528 GCGATTCATTGATGCCATCTA; CYP11A1-shRNA_#4–targeting sequence is
529 GAAATCCAACACCTCAGCGAT. Human HTR2C-shRNA–targeting sequence is
530 TCATGCACCTCTGCGCTATAT. Mouse HTR2C-shRNA–targeting sequence is . LacZ-
531 shRNA– targeting sequence is CTACACAAATCAGCGATT.

532

533 **Immunofluorescence**

534 Immunofluorescence microscopy assay was performed by previously described (ref).
535 Goat anti-mouse and goat anti-rabbit immunoglobulin G (IgG) antibodies conjugated to
536 Alexa Fluor 488 (Life Technologies) and diluted at 1:100 were used. Nuclei were
537 visualized by the addition of 2μg/ml of 4', 6-diamidino-2-phenylindole (DAPI) and
538 photographed at 100x magnification by a fluorescent microscope (Zeiss, Germany).

539

540 **Boyden chamber cell motility and invasion assay**

541 These assays were performed by previously described (16). In Boyden chamber assay,
542 either $3x10^5$ MDA-MB-231, $1x10^6$ MDA-MB-435, or $5x10^5$ PC9 cells were applied to
543 each well in the upper chamber.

544

545 **Zebrafish xenotransplantation model**

546 *Tg(kdrl:eGFP)* zebrafish was provided by Dr. Stainier (Max Planck Institute for Heart and
547 Lung Research). Embryos that were derived from the line were maintained in E3 medium
548 containing 200μM 1-phenyl-2-thiourea (PTU). Approximately 100-400 Red fluorescence
549 protein (RFP)-labelled MBA-MB-231 or MIA-Paca2 cells were injected into the duct of
550 Cuvier of the zebrafish at 2dpf.

551

552 **Spontaneous metastasis mouse model**

553 4T1-12B cells ($2x10^4$) were injected into the #4 mammary fat pad while the mice were
554 anesthetized. To monitor tumor growth and metastases, mice were imaged biweekly by
555 IVIS Imaging System (ParkinElmer). The primary tumor was resected 10 days after
556 inoculation. The study protocol (protocol number: BRC IACUC #110612) was approved
557 by A*STAR (Agency for Science, Technology and Research, Singapore).

558

559 **Histological Analysis**

560 All OCT embedded primary tumors, lungs, and livers of mice from the spontaneous
561 metastasis 4T1 model were sectioned on a cryostat. Eight micron sections were taken at
562 five hundred micron intervals through the entirety of the livers and lungs. Sections were
563 subsequently stained with hematoxylin and eosin. Metastatic lesions were counted under a
564 microscope in each section for both lungs and livers.

565

566 **Statistics**

567 Data were analyzed by Student's t test; $p < 0.05$ was considered significant.

568

569 **References**

570 1. Chambers AF, Groom AC, & MacDonald IC (2002) Dissemination and
571 growth of cancer cells in metastatic sites. *Nature reviews. Cancer* 2(8):563-
572 572.

573 2. Steeg PS (2003) Metastasis suppressors alter the signal transduction of
574 cancer cells. *Nature reviews. Cancer* 3(1):55-63.
575 3. Fidler IJ (2003) The pathogenesis of cancer metastasis: the 'seed and soil'
576 hypothesis revisited. *Nature reviews. Cancer* 3(6):453-458.
577 4. Cavallaro U & Christofori G (2004) Cell adhesion and signalling by
578 cadherins and Ig-CAMs in cancer. *Nature reviews. Cancer* 4(2):118-132.
579 5. Ellenbroek SI, Iden S, & Collard JG (2012) Cell polarity proteins and
580 cancer. *Semin Cancer Biol* 22(3):208-215.
581 6. Tsai JH & Yang J (2013) Epithelial-mesenchymal plasticity in carcinoma
582 metastasis. *Genes & development* 27(20):2192-2206.
583 7. Solnica-Krezel L (2005) Conserved patterns of cell movements during
584 vertebrate gastrulation. *Curr Biol* 15(6):R213-228.
585 8. Latimer A & Jessen JR (2010) Extracellular matrix assembly and
586 organization during zebrafish gastrulation. *Matrix Biol* 29(2):89-96.
587 9. Solnica-Krezel L (2006) Gastrulation in zebrafish -- all just about
588 adhesion? *Curr Opin Genet Dev* 16(4):433-441.
589 10. Tsai YJ, *et al.* (2011) The predominant protein arginine methyltransferase
590 PRMT1 is critical for zebrafish convergence and extension during
591 gastrulation. *FEBS J* 278(6):905-917.
592 11. Hsu HJ, Liang MR, Chen CT, & Chung BC (2006) Pregnenolone stabilizes
593 microtubules and promotes zebrafish embryonic cell movement. *Nature*
594 439(7075):480-483.
595 12. Weinbach EC & Garbus J (1969) Mechanism of Action of Reagents that
596 uncouple Oxidative Phosphorylation. *Nature* 221:1016.
597 13. Sack U, *et al.* (2011) Novel effect of antihelminthic Niclosamide on
598 S100A4-mediated metastatic progression in colon cancer. *Journal of the*
599 *National Cancer Institute* 103(13):1018-1036.
600 14. Huang EW, *et al.* (2012) Vinpocetine inhibits breast cancer cells growth in
601 vitro and in vivo. *Apoptosis : an international journal on programmed cell*
602 *death* 17(10):1120-1130.
603 15. Szilágyi G, *et al.* (2005) Effects of vinpocetine on the redistribution of
604 cerebral blood flow and glucose metabolism in chronic ischemic stroke
605 patients: a PET study. *Journal of the Neurological Sciences* 229-230:275-
606 284.
607 16. Nakayama J, Lu J, Makinoshima H, & Gong Z (2020) A Novel Zebrafish
608 Model of Metastasis Identifies the HSD11β1 Inhibitor Adrenosterone as a
609 Suppressor of Epithelial-Mesenchymal Transition and Metastatic
610 Dissemination. *Mol Cancer Res* 18(3):477-487.
611 17. Kolosionek E, *et al.* (2009) Expression and activity of phosphodiesterase
612 isoforms during epithelial mesenchymal transition: the role of
613 phosphodiesterase 4. *Mol Biol Cell* 20(22):4751-4765.
614 18. Sasaki T, *et al.* (2014) Serum CD10 is associated with liver metastasis in
615 colorectal cancer. *J Surg Res.* 192(2):390-394.
616 19. Liu P, *et al.* (2013) Disulfiram targets cancer stem-like cells and reverses
617 resistance and cross-resistance in acquired paclitaxel-resistant triple-
618 negative breast cancer cells. *British journal of cancer* 109(7):1876-1885.
619 20. Gunnarsson L, Jauhiainen A, Kristiansson E, Nerman O, & Larsson DGJ
620 (2008) Evolutionary conservation of human drug targets in organisms
621 used for environmental risk assessments. *Environmental Science &*
622 *Technology* 42(15):5807-5813.

21. Tao K, Fang M, Alroy J, & Sahagian GG (2008) Imagable 4T1 model for the study of late stage breast cancer. *BMC cancer* 8:228.
22. Kröger C, Afeyan, A.; Mraz, J.; Eaton, EN.; Reinhardt, F.; Khodor, YL.; Thiru, P.; Bierie B.; Ye, X.; Burge, CB.; Weinberg RA (2019) Acquisition of a hybrid E/M state is essential for tumorigenicity of basal breast cancer cells. *Proceedings of the National Academy of Sciences of the United States of America* 116(15):7353-7362.
23. Beyer TD, M.; Thumberger, T.; Vick, P.; Tisler, M.; Schneider, I.; Bogusch, S.; Andre, P.; Ulmer, B.; Walentek, P.; Niesler, B.; Blum, M.; Schweickert, A. (2012) Serotonin signaling is required for Wnt-dependent GRP specification and leftward flow in Xenopus. *Curr Biol* 22(1):33-39.
24. Sui HX, H.; Ji, Q.; Liu, X.; Zhou, L.; Song, H.; Zhou, X.; Xu, Y.; Chen, Z.; Cai, J.; Ji, G.; Li, Q. (2015) 5-hydroxytryptamine receptor (5-HT1DR) promotes colorectal cancer metastasis by regulating Axin1/β-catenin/MMP-7 signaling pathway. *Oncotarget* 6(28):25975-25987.
25. Zhan TR, N.; Boutros, M. (2017) Wnt signaling in cancer. *Oncogene* 36(11):1461–1473.
26. Nakayama J*, et al.* (2009) BLNK suppresses pre-B-cell leukemogenesis through inhibition of JAK3. *Blood* 113(7):1483-1492.

644 **Supplemental Information**

645

646 **Figure S1.**

647

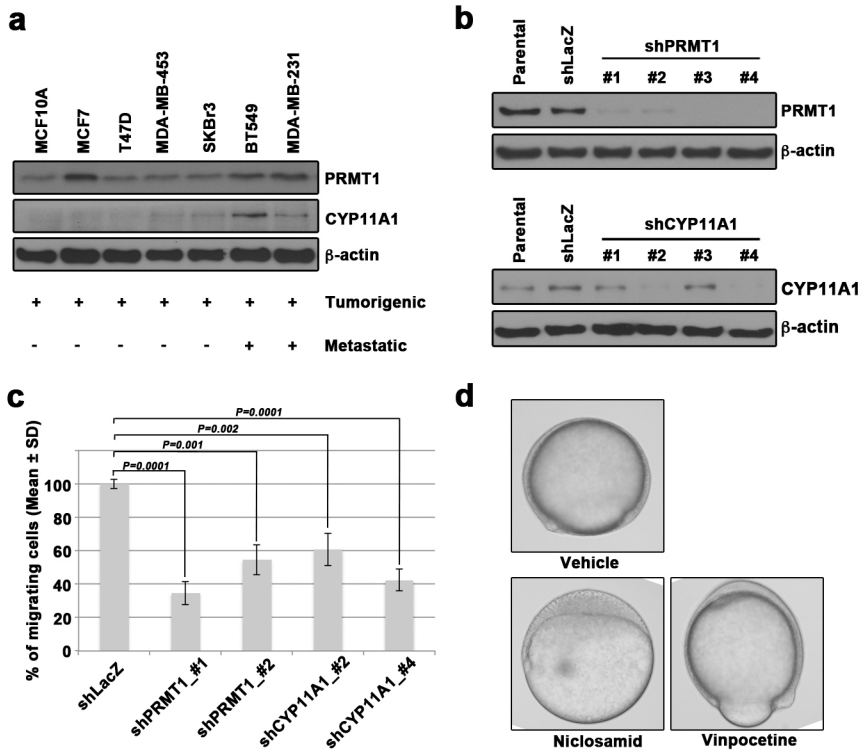

648

649

650 **Figure S1. Molecular mechanisms of epiboly in zebrafish overlap with those in**

651 **cancer metastasis.**

652 (A) Western blot analysis of PRMT1 (upper) and CYP11A1 (middle) protein levels in

653 non-metastatic human cancer cell lines, (MCF10, MCF7, MDA-MB-453, Sun159,

654 SKBr3) and highly metastatic human cancer cell lines, (BT549 and MDA-MB-231);

655 β-actin loading control is shown (bottom). (B) Knockdown of PRMT1 or CYP11A1

656 in MDA-MB-231 cells. MBA-MB-231 cells were transfected with a control shRNA

657 targeting LacZ, and one of four independent shRNAs targeting PRMT1 (clone #1 to

658 #4) or one of two independent shRNAs targeting CYP11A1 (clone #1 to #4). Reduced

659 PRMT1 and CYP11A1 expression, determined by western blot, in sub-cell lines of

660 MDA-MB-231 cells expressing PRMT1 shRNA (clone #3 and #4 or CYP11A1 (clone

661 #2 and #4), compared with controls (parental cell line MDA-MB-231 and control

662 shRNA cells); β-actin levels shown as a loading control. (C) Effect of shRNAs

663 targeting either PRMT1 or CYP11A1 on cell motility and invasion of MBA-MB-231
664 cells. Parental MDA-MB-231 cells and four sub-cell lines of MDA-MB-231 cells that
665 were transfected with either shRNA targeting either LacZ, two independent shRNAs
666 targeting PRMT1 (clone #3 and #4) or two independent shRNAs targeting CYP11A1
667 (clone #2 and #4), were subjected to Boyden chamber assays. (D) Zebrafish embryos
668 treated with either vehicle (DMSO), 10μM Niclosamide, or 50μM vinpocetine.
669 Approximately 20 embryos were treated with either DMSO as a vehicle control,
670 niclosamide, or vinpocetine. The treatment was started at 4 hpf when all of embryos
671 reached sphere stage and ended at 9 hpf when control embryos reached 80-90%
672 epiboly stage. Each experiment was performed at least twice. Statistical analysis was
673 determined by Student's *t* test.
674

675 **Figure S2.**

676

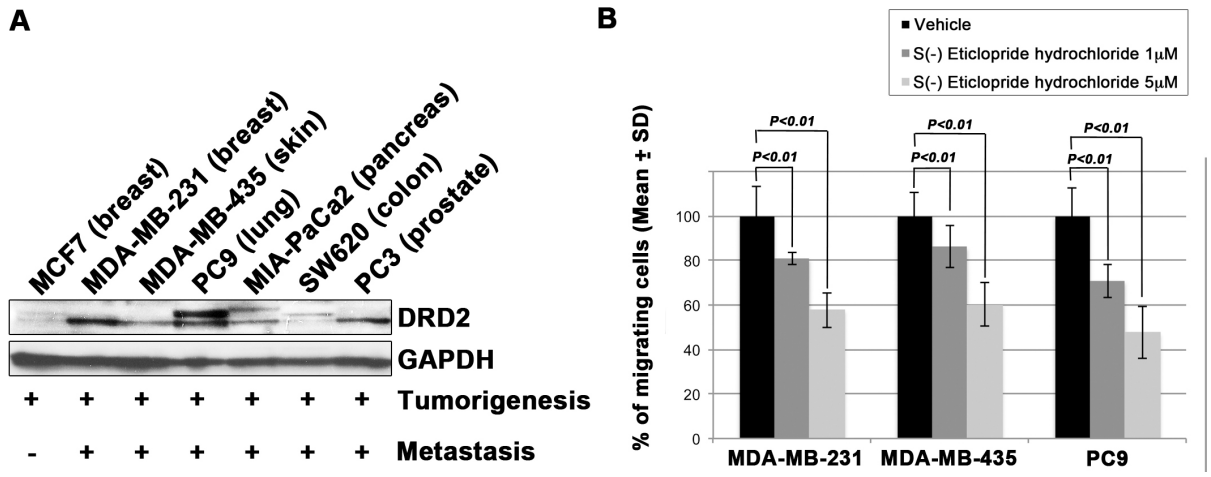

677

678

679 **Figure S2. S (-) Eticlopride hydrochloride suppressed cell motility and invasion of**

680 **human cancer cells.**

681 Related to Figure 2.

682 (A) Western blot analysis of DRD2 levels in non-metastatic human cancer cell line,

683 MCF7 (breast) and highly metastatic human cancer cell lines, MDA-MB-231 (breast),

684 MDA-MB-435 (melanoma), MIA-PaCa2 (pancreas), PC3 (prostate) and SW620 (colon);

685 GAPDH loading control is shown (bottom). (B) Effect of S (-) Eticlopride hydrochloride

686 on cell motility and invasion of MBA-MB-231, MDA-MB-435, and PC9 cells. Either

687 vehicle or pizotifen treated cells were subjected to Boyden chamber assays. Fetal bovine

688 serum (1%v/v) was used as the chemoattractant in both assays. Each experiment was

689 performed at least twice. Statistical analysis was determined by Student's *t* test.

690

691 **Figure S3.**

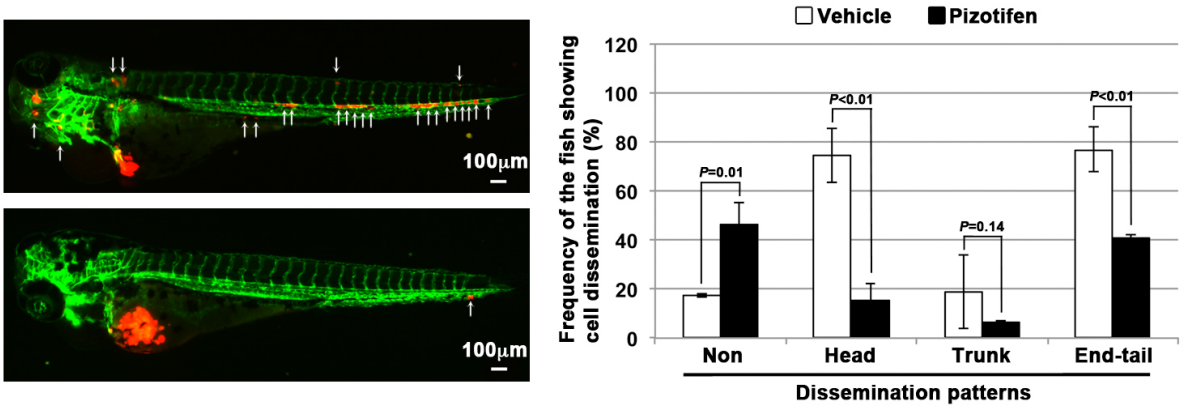

692

693 **Figure S3. Pizotifen suppressed metastatic dissemination of human pancreatic**

694 **cancer cells in a zebrafish xenotransplantation model.**

695 Related to Figure 2.

696 Representative images of dissemination of MIA-PaCa2 cells in zebrafish

697 xenotransplantation model. The fish were inoculated with MIA-PaCa2 cells, and treated

698 with either vehicle (top left) or drug (lower left). White arrows heads indicate

699 disseminated MIA-PaCa2 cells. The images were shown in 4x magnification. Scale bar,

700 100μm. The mean frequencies of the fish showing head, trunk, or end-tail dissemination

701 were tabulated (right). Each value is indicated as the mean ± SEM of two independent

702 experiments. Statistical analysis was determined by Student's *t* test.

703

704 **Table S1. A list of the genes that are involved between gastrulation and**
705 **metastasis progression**
706

Genes	Gastrulation Defects	Ref	Effects in Metastasis	Ref
BMP	Convergence and extension	(1)	EMT	(2)
WNT	Convergence and extension	(3)	Migration and Invasion	(4)
FGF	Convergence and extension	(5)	Invision	(6)
EGF	Epiboly	(7)	Migration	(8)
PDGF	Convergence and extension	(9)	EMT	(10)
CXCL12	Migration of endodermal cells	(11)	Migration and Invasion	(12)
CXCR4	Migration of endodermal cells	(11)	Migration and Invasion	(12)
PIK3CA	Convergence and extension	(13)	Migration and Invasion	(14)
YES	Epiboly	(15)	Migration	(16)
FYN	Epiboly	(17)	Migration and Invasion	(18)
MAPK1	Epiboly	(19)	Migration	(20)
SHP2	Convergence and extension	(21)	Migration	(22)
SNAI1	Convergence and extension	(23)	EMT	(24)
SNAI2	Mesoderm & Neural crest formation	(25)	EMT	
TWIST1	Mesoderm formation	(26)	EMT	(27)
TBXT	Convergence and extension	(3)	EMT	(28)
ZEB1	Epiboly	(29)	EMT	(30)
GSC	Mesodermal patterning	(31)	EMT	(32)
FOXC2	Unclear, defects in gastrulation	(33)	EMT	(34)
STAT3	Convergence and extension	(35)	Migration	(36)
POU5F1	Epiboly	(37)	EMT	(38)
EZH2	Unclear, defects in gastrulation	(39)	Invasion	(40)
EHMT2	Defects in Neurogenesis	(41)	Migration and Invasion	(42)
BMI1	Defects in skelton formation	(43)	EMT	(44)
RHOA	Convergence and extension	(45)	Migration and Invasion	(46)
CDC42	Convergence and extension	(47)	Migration and Invasion	(48)
RAC1	Convergence and extension	(49)	Migration and Invasion	(50)
ROCK2	Convergence and extension	(51)	Migration and Invasion	(52)
PAR1	Convergence and extension	(53)	Migration	(54)
PRKCI	Convergence and extension	(53)	EMT	(55)
CAP1	Convergence and extension	(56)	Migration	(57)
EZR	Epiboly	(58)	Migration	(59)
EPCAM	Epiboly	(60)	Migration and Invasion	(61)
ITGB1 / ITA5	Mesodermal Migration	(62)	Migration and Invasion	(63)
FN1	Convergence and extension	(64)	Invasion	(65)
HAS2	Dorsal migration of lateral cells	(66)	Invasion	(67)
MMP14	Convergence and extension	(68)	Invasion	(69)
COX1	Epiboly	(70)	Invasion	(71)
PTGES	Convergence and extension	(72)	Invasion	(73)
SLC39A6	Aterior migration	(74)	EMT	(75)
GNA12 / 13	Convergence and extension	(41)	Migration and Invasion	(76)
OGT	Epiboly	(77)	Migration and Invasion	(78)
CCN1	Cell Movement	(79)	Migration and Invasion	(80)
TRPM7	Convergence and extension	(81)	Migration	(82)
MAPKAPK2	Epiboly	(83)	Migration	(84)
B4GALT1	Convergence and extension	(85)	Invasion	(86)
IER2	Convergence and extension	(87)	Migration	(88)
TIP1	Convergence and extension	(89)	Migration and Invasion	(90)
PAK5	Convergence and extension	(91)	Migration	(92)
MARCKS	Convergence and extension	(93)	Migration and Invasion	(94)

707

708 **Table S1.**

709 A list of the fifty genes that play essential role in governing both metastasis and

710 gastrulation progression. The gastrulation defects in Xenopus or zebrafish that are

711 induced by knockdown of each of these genes, were indicated. The molecular

712 mechanism in metastasis that are inhibited by knockdown of each of the same genes,

713 were indicated.

714 **Table S2. A list of the drugs that interfere with epiboly progression in zebrafish**
715

Chemical name	Chemical formula	Effect of 10uM	Effect of 50uM
Acitretin	C21H26O3	Delayed	Delayed
Adrenosterone	C19H24O3	Delayed	Delayed
Albendazole	C12H15N3O2S	Severe delayed	Severe delayed
Alfadolone acetate	C23H34O5	Delayed	Delayed
Alfaxalone	C21H32O3	Delayed	Delayed
Alprostadil	C20H34O5	Delayed	Delayed
Altrenogest	C21H26O2	Slightly delayed	Delayed
Ampiroxicam	C20H21N3O7S	Non effect	Delayed
Anethole-trithione	C10H8OS3	Delayed	Delayed
Antimycin A	C28H40N2O9	Delayed	Delayed
Avobenzone	C20H22O3	Delayed	Delayed
Benzoxiquine	C16H11NO2	Non effect	Delayed
Bosentan	C27H29N5O6S	Delayed	Delayed
Butoconazole nitrate	C19H18Cl3N3O3S	Delayed	Toxic lethal
Camptothecine (S,+)	C20H16N2O4	Severe delayed	Severe delayed
Carbenoxolone disodium salt	C34H48Na2O7	Delayed	Toxic lethal
Carmofur	C11H16FN3O3	Slightly delayed	Delayed
Carprofen	C15H12ClNO2	Severe delayed	Toxic lethal
Cefdinir	C14H13N5O5S2	Delayed	Delayed
Celecoxib	C17H14F3N3O2S	Delayed	Delayed
Chlorambucil	C14H19Cl2NO2	Slightly delayed	Delayed
Chlorhexidine	C22H30Cl2N10	Non effect	Toxic lethal
Ciclopirox ethanolamine	C14H24N2O3	Delayed	Severe delayed
Cinoxacin	C12H10N2O5	Delayed	Severe delayed
Clofibrate	C12H15ClO3	Non effect	Severe delayed
Clopidogrel	C16H16ClNO2S	Non effect	Delayed
Clorgyline hydrochloride	C13H16Cl3NO	Delayed	Delayed
Colchicine	C22H25NO6	Non effect	Delayed
Deptropine citrate	C29H35NO8	Delayed	Delayed
Desipramine hydrochloride	C18H23ClN2	Delayed	Delayed
Diclofenac sodium	C14H10Cl2NNaO2	Delayed	Severe delayed
Dicumarol	C19H12O6	Delayed	Severe delayed
Diethylstilbestrol	C18H20O2	Delayed	Toxic lethal
Dimaprit dihydrochloride	C6H17Cl2N3S	Slightly delayed	Delayed
Disulfiram	C10H20N2S4	Delayed	Delayed
Dopamine hydrochloride	C8H12ClNO2	Delayed	Delayed
Eburnamonine (-)	C19H22N2O	Delayed	Delayed
Ethaverine hydrochloride	C24H30ClNO4	Delayed	Delayed
Ethinylestradiol	C20H24O2	Delayed	Severe delayed
Ethopropazine hydrochloride	C19H25ClN2S	Delayed	Delayed
Ethoxyquin	C14H19NO	Non effect	Delayed
Exemestane	C20H24O2	Slightly delayed	Delayed
Ezetimibe	C24H21F2NO3	Slightly delayed	Delayed
Fenbendazole	C15H13N3O2S	Non effect	Delayed
Fenoprofen calcium salt dihydrate	C30H30CaO8	Slightly delayed	Delayed
Fentiazac	C17H12ClNO2S	Toxic lethal	Toxic lethal
Floxuridine	C9H11FN2O5	Delayed	Toxic lethal
Flunixin meglumine	C21H28F3N3O7	Delayed	Toxic lethal
Flutamide	C11H11F3N2O3	Delayed	Toxic lethal
Fluticasone propionate	C25H31F3O5S	Non effect	Delayed
Furosemide	C12H11ClN2O5S	Delayed	Delayed
Gatifloxacin	C19H22FN3O4	Delayed	Delayed
Gemcitabine	C9H11F2N3O4	Delayed	Delayed
Gemfibrozil	C15H22O3	Delayed	Toxic lethal
Gestrinone	C21H24O2	Delayed	Delayed
Haloprogin	C9H4Cl3IO	Delayed	Toxic lethal
Hexachlorophene	C13H6Cl6O2	Delayed	Severe delayed
Hexestrol	C18H22O2	Slightly delayed	Delayed
Ibudilast	C14H18N2O	Non effect	Delayed
Idazoxan hydrochloride	C11H13ClN2O2	Slightly delayed	Delayed
Idazoxan hydrochloride	C11H13ClN2O2	Non effect	Delayed

Idebenone	C19H30O5	Severe delayed	Toxic lethal
Indomethacin	C19H16ClNO4	Non effect	Delayed
Ipriflavone	C18H16O3	Delayed	Severe delayed
Isotretinoin	C20H28O2	Non effect	Severe delayed
Isradipine	C19H21N3O5	Non effect	Delayed
Lansoprazole	C16H14F3N3O2S	Slightly delayed	Delayed
Latanoprost	C26H40O5	Non effect	Delayed
Leflunomide	C12H9F3N2O2	Delayed	Severe delayed
Letrozole	C17H11N5	Non effect	Delayed
Lithocholic acid	C24H40O3	Non effect	Delayed
Lodoxamide	C11H6ClN3O6	Non effect	Delayed
Lofepramine	C26H27ClN2O	Non effect	Delayed
Loratadine	C22H23ClN2O2	Delayed	Delayed
Loxapine succinate	C22H24ClN3O5	Delayed	Delayed
Mebendazole	C16H13N3O3	Severe delayed	Severe delayed
Mebendazole	C22H26N2O2	Non effect	Delayed
Meloxicam	C14H13N3O4S2	Delayed	Toxic lethal
Methiazole	C12H15N3O2S	Delayed	Delayed
Mevastatin	C23H34O5	Non effect	Delayed
MK 801 hydrogen maleate	C20H19NO4	Slightly delayed	Delayed
Nabumetone	C15H16O2	Non effect	Severe delayed
Naftopidil dihydrochloride	C24H30Cl2N2O3	Slightly delayed	Delayed
Nandrolone	C18H26O2	Delayed	Delayed
Naproxen sodium salt	C14H13NaO3	Delayed	Delayed
Niclosamide	C13H8Cl2N2O4	Delayed	Delayed
Nifekalant	C19H27N5O5	Delayed	Delayed
Niflumic acid	C13H9F3N2O2	Delayed	Delayed
Nimesulide	C13H12N2O5S	Non effect	Delayed
Nisoldipine	C20H24N2O6	Delayed	Toxic lethal
Nitazoxanide	C12H9N3O5S	Severe delayed	Severe delayed
Norethindrone	C20H26O2	Non effect	Delayed
Norgestimate	C23H31NO3	Slightly delayed	Delayed
Oxfendazol	C15H13N3O3S	Slightly delayed	Delayed
Oxibendazol	C12H15N3O3	Severe delayed	Severe delayed
Oxymetholone	C21H32O3	Slightly delayed	Delayed
Parbendazole	C13H17N3O2	Severe delayed	Severe delayed
Parthenolide	C15H20O3	Non effect	Delayed
Penciclovir	C10H15N5O3	Non effect	Delayed
Pentobarbital	C11H18N2O3	Non effect	Delayed
Phenazopyridine hydrochloride	C11H12ClN5	Delayed	Toxic lethal
Phenothiazine	C12H9NS	Non effect	Delayed
Phenoxybenzamine hydrochloride	C18H23Cl2NO	Non effect	Delayed
Pizotifen malate	C23H27NO5S	Delayed	Severe delayed
Pramoxine hydrochloride	C17H28ClNO3	Slightly delayed	Delayed
Prilocaine hydrochloride	C13H21ClN2O	Non effect	Delayed
Primidone	C12H14N2O2	Slightly delayed	Delayed
Racecadotril	C21H23NO4S	Slightly delayed	Delayed
Riluzole hydrochloride	C8H6ClF3N2OS	Non effect	Delayed
Ritonavir	C37H48N6O5S2	Non effect	Severe delayed
S(-)Eticlopride hydrochloride	C17H26Cl2N2O3	Delayed	Delayed
Salmeterol	C25H37NO4	Non effect	Delayed
Streptomycin sulfate	C42H84N14O36S3	Non effect	Delayed
Sulconazole nitrate	C18H16Cl3N3O3S	Delayed	Delayed
Tegafur	C8H9FN2O3	Delayed	Delayed
Telmisartan	C33H30N4O2	Severe delayed	Toxic lethal
Tenatoprazole	C16H18N4O3S	Non effect	Delayed
Terbinafine	C21H25N	Non effect	Delayed
Thimerosal	C9H9HgNaO2S	Non effect	Delayed
Thiorphan	C12H15NO3S	Delayed	Delayed
Tolcapone	C14H11NO5	Severe delayed	Severe delayed
Topotecan	C23H23N3O5	Delayed	Delayed
Tracazolate hydrochloride	C16H25ClN4O2	Severe delayed	Delayed
Tribenoside	C29H34O6	Delayed	Delayed
Triclabendazole	C14H9Cl3N2OS	Delayed	Delayed
Triclosan	C12H7Cl3O2	Delayed	Severe delayed

Trioxsalen	C14H12O3	Delayed	Delayed
Troglitazone	C24H27NO5S	Severe delayed	Toxic lethal
Valproic acid	C8H16O2	Non effect	Delayed
Voriconazole	C16H14F3N5O	Non effect	Delayed
Zardaverine	C12H10F2N2O3	Slightly delayed	Delayed
Zuclopenthixol dihydrochloride	C22H27Cl3N2OS	Delayed	Delayed

716

717 **Table S2. A list of the drugs that interfere with epiboly progression in zebrafish.**

718 Related to Figure 1.

719 A list of positive "hit" drugs that interfered with epiboly progression. Gastrulation

720 defects or status of each of the zebrafish embryos that were treated with either 10μM

721 or 50μM concentrations, are indicated.

722

723 **References for Table S1.**

724 1. Kondo M (2007) Bone morphogenetic proteins in the early development
725 of zebrafish. *FEBS J* 274(12):2960-2967.
726 2. Katsuno Y, *et al.* (2008) Bone morphogenetic protein signaling enhances
727 invasion and bone metastasis of breast cancer cells through Smad
728 pathway. *Oncogene* 27(49):6322-6333.
729 3. Tada M & Smith JC (2000) Xwnt11 is a target of Xenopus Brachyury:
730 regulation of gastrulation movements via Dishevelled, but not through the
731 canonical Wnt pathway. *Development* 127:2227-2238.
732 4. Vincan E & Barker N (2008) The upstream components of the Wnt
733 signalling pathway in the dynamic EMT and MET associated with
734 colorectal cancer progression. *Clin Exp Metastasis* 25(6):657-663.
735 5. Yang X, Dormann D, Munsterberg AE, & Weijer CJ (2002) Cell movement
736 patterns during gastrulation in the chick are controlled by positive and
737 negative chemotaxis mediated by FGF4 and FGF8. *Dev Cell* 3(3):425-437.
738 6. Nomura S, *et al.* (2008) FGF10/FGFR2 signal induces cell migration and
739 invasion in pancreatic cancer. *Br J Cancer* 99(2):305-313.
740 7. Song S, *et al.* (2013) Pou5f1-dependent EGF expression controls E-
741 cadherin endocytosis, cell adhesion, and zebrafish epiboly movements.
742 *Dev Cell* 24(5):486-501.
743 8. Lu Z, Jiang G, Blume-Jensen P, & Hunter T (2001) Epidermal growth
744 factor-induced tumor cell invasion and metastasis initiated by
745 dephosphorylation and downregulation of focal adhesion kinase. *Mol Cell*
746 *Biol* 21(12):4016-4031.
747 9. Damm EW & Winklbauer R (2011) PDGF-A controls mesoderm cell
748 orientation and radial intercalation during Xenopus gastrulation.
749 *Development* 138(3):565-575.
750 10. Jechlinger M, *et al.* (2006) Autocrine PDGFR signaling promotes mammary
751 cancer metastasis. *J Clin Invest* 116(6):1561-1570.
752 11. Mizoguchi T, Verkade H, Heath JK, Kuroiwa A, & Kikuchi Y (2008)
753 Sdf1/Cxcr4 signaling controls the dorsal migration of endodermal cells
754 during zebrafish gastrulation. *Development* 135(15):2521-2529.

755 12. Shen HB, Gu ZQ, Jian K, & Qi J (2013) CXCR4-mediated Stat3 activation is
756 essential for CXCL12-induced cell invasion in bladder cancer. *Tumour Biol*
757 34(3):1839-1845.
758 13. Montero J-A, Kilian B, Chan J, Bayliss PE, & Heisenberg C-P (2003)
759 Phosphoinositide 3-Kinase Is Required for Process Outgrowth and Cell
760 Polarization of Gastrulating Mesendodermal Cells. *Current Biology*
761 13(15):1279-1289.
762 14. Wander SA*, et al.* (2013) PI3K/mTOR inhibition can impair tumor
763 invasion and metastasis in vivo despite a lack of antiproliferative action in
764 vitro: implications for targeted therapy. *Breast Cancer Res Treat*
765 138(2):369-381.
766 15. Tsai WB, Zhang X, Sharma D, Wu W, & Kinsey WH (2005) Role of Yes
767 kinase during early zebrafish development. *Dev Biol* 277(1):129-141.
768 16. Barraclough J, Hodgkinson C, Hogg A, Dive C, & Welman A (2007)
769 Increases in c-Yes Expression Level and Activity Promote Motility But Not
770 Proliferation of Human Colorectal Carcinoma Cells. *Neoplasia* 9(9):745-
771 IN732.
772 17. Sharma D, Holets L, Zhang X, & Kinsey WH (2005) Role of Fyn kinase in
773 signaling associated with epiboly during zebrafish development. *Dev Biol*
774 285(2):462-476.
775 18. Yadav V & Denning MF (2011) Fyn is induced by Ras/PI3K/Akt signaling
776 and is required for enhanced invasion/migration. *Mol Carcinog* 50(5):346-
777 352.
778 19. Krens SF*, et al.* (2008) Distinct functions for ERK1 and ERK2 in cell
779 migration processes during zebrafish gastrulation. *Dev Biol* 319(2):370-
780 383.
781 20. Radtke S, Milanovic M, & Rossé C (2013) ERK2 but not ERK1 mediates
782 HGF-induced motility in non-small cell lung carcinoma cell lines. *J Cell Sci.*
783 126(Pt11):2381-2391.
784 21. Jopling C, van Geemen D, & den Hertog J (2007) Shp2 knockdown and
785 Noonan/LEOPARD mutant Shp2-induced gastrulation defects. *PLoS Genet*
786 3(12):e225.
787 22. Wang FM*, et al.* (2005) SHP-2 promoting migration and metastasis of
788 MCF-7 with loss of E-cadherin, dephosphorylation of FAK and secretion of
789 MMP-9 induced by IL-1beta in vivo and in vitro. *Breast Cancer Res Treat*
790 89(1):5-14.
791 23. Ip YT & Gridley T (2002) Cell movements during gastrulation: snail
792 dependent and independent pathways. *Curr Opin Genet Dev* 12(4):423-
793 429.
794 24. Batlle E, Sancho E, Francí C, Domínguez D, & Monfar M (2000) The
795 transcription factor snail is a repressor of E-cadherin gene expression in
796 epithelial tumour cells. *Nat Cell Biol* 2(2):84-89.
797 25. Shi J, Severson C, Yang J, Wedlich D, & Klymkowsky MW (2011) Snail2
798 controls mesodermal BMP/Wnt induction of neural crest. *Development*
799 138(15):3135-3145.
800 26. Castanon I & Baylies MK (2002) A Twist in fate: evolutionary comparison
801 of Twist structure and function. *Gene* 287(1-2):11-22.
802 27. Yang J*, et al.* (2004) Twist, a master regulator of morphogenesis, plays an
803 essential role in tumor metastasis. *Cell* 117(7):927-939.

804 28. Fernando RI, *et al.* (2010) The T-box transcription factor Brachyury
805 promotes epithelial-mesenchymal transition in human tumor cells. *J Clin*
806 *Invest* 120(2):533-544.
807 29. Vannier C, Mock K, Brabletz T, & Driever W (2013) Zeb1 regulates E-
808 cadherin and Epcam (epithelial cell adhesion molecule) expression to
809 control cell behavior in early zebrafish development. *J Biol Chem*
810 288(26):18643-18659.
811 30. Spaderna S, *et al.* (2008) The transcriptional repressor ZEB1 promotes
812 metastasis and loss of cell polarity in cancer. *Cancer Res* 68(2):537-544.
813 31. Sander V, Reversade B, & De Robertis EM (2007) The opposing homeobox
814 genes Goosecoid and Vent1/2 self-regulate Xenopus patterning. *EMBO J*
815 26(12):2955-2965.
816 32. Hartwell KA, *et al.* (2006) The Spemann organizer gene, Goosecoid,
817 promotes tumor metastasis. *Proc Natl Acad Sci U S A* 103(50):18969-
818 18974.
819 33. Wilm B, James RG, Schultheiss TM, & Hogan BL (2004) The forkhead
820 genes, Foxc1 and Foxc2, regulate paraxial versus intermediate mesoderm
821 cell fate. *Dev Biol* 271(1):176-189.
822 34. Mani SA, *et al.* (2007) Mesenchyme Forkhead 1 (FOXC2) plays a key role
823 in metastasis and is associated with aggressive basal-like breast cancers.
824 *Proc Natl Acad Sci U S A* 104(24):10069-10074.
825 35. Miyagi C, *et al.* (2004) STAT3 noncell-autonomously controls planar cell
826 polarity during zebrafish convergence and extension. *J Cell Biol*
827 166(7):975-981.
828 36. Abdulghani J, *et al.* (2008) Stat3 promotes metastatic progression of
829 prostate cancer. *Am J Pathol* 172(6):1717-1728.
830 37. Lachnit M, Kur E, & Driever W (2008) Alterations of the cytoskeleton in all
831 three embryonic lineages contribute to the epiboly defect of Pou5f1/Oct4
832 deficient MZspg zebrafish embryos. *Dev Biol* 315(1):1-17.
833 38. Dai X, *et al.* (2013) OCT4 regulates epithelial-mesenchymal transition and
834 its knockdown inhibits colorectal cancer cell migration and invasion.
835 *Oncol Rep* 29(1):155-160.
836 39. O'Carroll D, *et al.* (2001) The polycomb-group gene Ezh2 is required for
837 early mouse development. *Mol Cell Biol* 21(13):4330-4336.
838 40. Ren G, *et al.* (2012) Polycomb protein EZH2 regulates tumor invasion via
839 the transcriptional repression of the metastasis suppressor RKIP in breast
840 and prostate cancer. *Cancer Res* 72(12):3091-3104.
841 41. Lin F, *et al.* (2005) Essential roles of G{alpha}12/13 signaling in distinct
842 cell behaviors driving zebrafish convergence and extension gastrulation
843 movements. *J Cell Biol* 169(5):777-787.
844 42. Chen MW, *et al.* (2010) H3K9 histone methyltransferase G9a promotes
845 lung cancer invasion and metastasis by silencing the cell adhesion
846 molecule Ep-CAM. *Cancer Res* 70(20):7830-7840.
847 43. van der Lugt NM, *et al.* (1994) Posterior transformation, neurological
848 abnormalities, and severe hematopoietic defects in mice with a targeted
849 deletion of the bmi-1 proto-oncogene. *Genes Dev* 8(7):757-769.
850 44. Guo BH, *et al.* (2011) Bmi-1 promotes invasion and metastasis, and its
851 elevated expression is correlated with an advanced stage of breast cancer.
852 *Mol Cancer* 10(1):10.
853 45. Zhu S, Liu L, Korzh V, Gong Z, & Low BC (2006) RhoA acts downstream of
854 Wnt5 and Wnt11 to regulate convergence and extension movements by

855 involving effectors Rho kinase and Diaphanous: use of zebrafish as an in
856 vivo model for GTPase signaling. *Cell Signal* 18(3):359-372.
857 46. Yoshioka K, Nakamori S, & Itoh K (1999) Overexpression of small GTP-
858 binding protein RhoA promotes invasion of tumor cells. *Cancer Res*
859 59(8):2004-2010.
860 47. Choi SC & Han JK (2002) Xenopus Cdc42 regulates convergent extension
861 movements during gastrulation through Wnt/Ca2+ signaling pathway.
862 *Dev Biol* 244(2):342-357.
863 48. Reymond N*, et al.* (2012) Cdc42 promotes transendothelial migration of
864 cancer cells through beta1 integrin. *J Cell Biol* 199(4):653-668.
865 49. Habas R, Dawid IB, & He X (2003) Coactivation of Rac and Rho by
866 Wnt/Frizzled signaling is required for vertebrate gastrulation. . *Genes Dev*
867 17(2):295-309.
868 50. Vega FM & Ridley AJ (2008) Rho GTPases in cancer cell biology. *FEBS Lett*
869 582(14):2093-2101.
870 51. Marlow F, Topczewski J, Sepich D, & Solnica-Krezel L (2002) Zebrafish
871 Rho kinase 2 acts downstream of Wnt11 to mediate cell polarity and
872 effective convergence and extension movements. *Curr Biol* 12(11):876-
873 884.
874 52. Itoh K*, et al.* (1999) An essential part for Rho-associated kinase in the
875 transcellular invasion of tumor cells. *Nat Med* 5(2):221-225.
876 53. Kusakabe M & Nishida E (2004) The polarity-inducing kinase Par-1
877 controls Xenopus gastrulation in cooperation with 14-3-3 and aPKC.
878 *EMBO J* 23(21):4190-4201.
879 54. Shi X, Gangadharan B, Brass LF, Ruf W, & Mueller BM (2004) Protease-
880 activated receptors (PAR1 and PAR2) contribute to tumor cell motility
881 and metastasis. *Mol Cancer Res* 2(7):395-402.
882 55. Gunaratne A, Thai BL, & Di Guglielmo GM (2013) Atypical protein kinase C
883 phosphorylates Par6 and facilitates transforming growth factor beta-
884 induced epithelial-to-mesenchymal transition. *Mol Cell Biol* 33(5):874-
885 886.
886 56. Seifert K, Ibrahim H, Stodtmeister T, Winklbauer R, & Niessen CM (2009)
887 An adhesion-independent, aPKC-dependent function for cadherins in
888 morphogenetic movements. *J Cell Sci* 122(Pt 14):2514-2523.
889 57. Yamazaki K*, et al.* (2009) Adenylate cyclase-associated protein 1
890 overexpressed in pancreatic cancers is involved in cancer cell motility.
891 *Lab Invest* 89(4):425-432.
892 58. Link V*, et al.* (2006) Identification of regulators of germ layer
893 morphogenesis using proteomics in zebrafish. *J Cell Sci* 119(Pt 10):2073-
894 2083.
895 59. Khanna C*, et al.* (2004) The membrane-cytoskeleton linker ezrin is
896 necessary for osteosarcoma metastasis. *Nat Med* 10(2):182-186.
897 60. Slanchev K*, et al.* (2009) The epithelial cell adhesion molecule EpCAM is
898 required for epithelial morphogenesis and integrity during zebrafish
899 epiboly and skin development. *PLoS Genet* 5(7):e1000563.
900 61. Ni J*, et al.* (2012) Role of the EpCAM (CD326) in prostate cancer
901 metastasis and progression. *Cancer Metastasis Rev* 31(3-4):779-791.
902 62. Skalski M, Alfandari D, & Darribere T (1998) A key function for alphav
903 containing integrins in mesodermal cell migration during Pleurodeles
904 waltl gastrulation. *Dev Biol* 195(2):158-173.

905 63. Felding-Habermann B (2003) Integrin adhesion receptors in tumor
906 metastasis. *Clin Exp Metastasis* 20(3):203-213.
907 64. Marsden M & DeSimone DW (2003) Integrin-ECM Interactions Regulate
908 Cadherin-Dependent Cell Adhesion and Are Required for Convergent
909 Extension in Xenopus. *Current Biology* 13(14):1182-1191.
910 65. Malik G, *et al.* (2010) Plasma fibronectin promotes lung metastasis by
911 contributions to fibrin clots and tumor cell invasion. *Cancer Res*
912 70(11):4327-4334.
913 66. Bakkers J, *et al.* (2004) Has2 is required upstream of Rac1 to govern
914 dorsal migration of lateral cells during zebrafish gastrulation.
915 *Development* 131(3):525-537.
916 67. Kim HR, *et al.* (2004) Hyaluronan facilitates invasion of colon carcinoma
917 cells in vitro via interaction with CD44. *Cancer Res* 64(13):4569-4576.
918 68. Coyle RC, Latimer A, & Jessen JR (2008) Membrane-type 1 matrix
919 metalloproteinase regulates cell migration during zebrafish gastrulation:
920 evidence for an interaction with non-canonical Wnt signaling. *Exp Cell Res*
921 314(10):2150-2162.
922 69. Perentes JY, *et al.* (2011) Cancer cell-associated MT1-MMP promotes
923 blood vessel invasion and distant metastasis in triple-negative mammary
924 tumors. *Cancer Res* 71(13):4527-4538.
925 70. Cha YI, *et al.* (2006) Cyclooxygenase-1-derived PGE2 promotes cell
926 motility via the G-protein-coupled EP4 receptor during vertebrate
927 gastrulation. *Genes Dev* 20(1):77-86.
928 71. Kundu N & Fulton AM (2002) Selective cyclooxygenase (COX)-1 or COX-2
929 inhibitors control metastatic disease in a murine model of breast cancer.
930 *Cancer Res* 62(8):2343-2346.
931 72. Speirs CK, *et al.* (2010) Prostaglandin Gbetagamma signaling stimulates
932 gastrulation movements by limiting cell adhesion through Snai1a
933 stabilization. *Development* 137(8):1327-1337.
934 73. Wang D & Dubois RN (2006) Prostaglandins and cancer. *Gut* 55(1):115-
935 122.
936 74. Yamashita S, *et al.* (2004) Zinc transporter LIVI controls epithelial-
937 mesenchymal transition in zebrafish gastrula organizer. *Nature*
938 429(6989):298-302.
939 75. Lue HW, *et al.* (2011) LIV-1 promotes prostate cancer epithelial-to-
940 mesenchymal transition and metastasis through HB-EGF shedding and
941 EGFR-mediated ERK signaling. *PLoS One* 6(11):e27720.
942 76. Yagi H, *et al.* (2011) A synthetic biology approach reveals a CXCR4-G13-
943 Rho signaling axis driving transendothelial migration of metastatic breast
944 cancer cells. *Sci Signal* 4(191):ra60.
945 77. Webster DM, *et al.* (2009) O-GlcNAc modifications regulate cell survival
946 and epiboly during zebrafish development. *BMC Dev Biol* 9:28.
947 78. Lynch TP, *et al.* (2012) Critical role of O-Linked beta-N-acetylglucosamine
948 transferase in prostate cancer invasion, angiogenesis, and metastasis. *J*
949 *Biol Chem* 287(14):11070-11081.
950 79. Latinkic BV (2003) Xenopus Cyr61 regulates gastrulation movements and
951 modulates Wnt signalling. *Development* 130(11):2429-2441.
952 80. Lin J, *et al.* (2012) A novel anti-Cyr61 antibody inhibits breast cancer
953 growth and metastasis in vivo. *Cancer Immunol Immunother* 61(5):677-
954 687.

955 81. Liu W, *et al.* (2011) TRPM7 regulates gastrulation during vertebrate
956 embryogenesis. *Dev Biol* 350(2):348-357.
957 82. Middelbeek J, *et al.* (2012) TRPM7 is required for breast tumor cell
958 metastasis. *Cancer Res* 72(16):4250-4261.
959 83. Holloway BA, *et al.* (2009) A novel role for MAPKAPK2 in morphogenesis
960 during zebrafish development. *PLoS Genet* 5(3):e1000413.
961 84. Kumar B, *et al.* (2010) p38 mitogen-activated protein kinase-driven
962 MAPKAPK2 regulates invasion of bladder cancer by modulation of MMP-2
963 and MMP-9 activity. *Cancer Res* 70(2):832-841.
964 85. Machingo QJ, Fritz A, & Shur BD (2006) A beta1,4-galactosyltransferase is
965 required for convergent extension movements in zebrafish. *Dev Biol*
966 297(2):471-482.
967 86. Zhu X, *et al.* (2005) Elevated beta1,4-galactosyltransferase I in highly
968 metastatic human lung cancer cells. Identification of E1AF as important
969 transcription activator. *J Biol Chem* 280(13):12503-12516.
970 87. Hong SK, Tanegashima K, & Dawid IB (2011) XIer2 is required for
971 convergent extension movements during Xenopus development. *Int J Dev*
972 *Biol* 55(10-12):917-921.
973 88. Neeb A, *et al.* (2012) The immediate early gene Ier2 promotes tumor cell
974 motility and metastasis, and predicts poor survival of colorectal cancer
975 patients. *Oncogene* 31(33):3796-3806.
976 89. Besser J, Leito JT, van der Meer DL, & Bagowski CP (2007) Tip-1 induces
977 filopodia growth and is important for gastrulation movements during
978 zebrafish development. *Dev Growth Differ* 49(3):205-214.
979 90. Han M, Wang H, Zhang HT, & Han Z (2012) The PDZ protein TIP-1
980 facilitates cell migration and pulmonary metastasis of human invasive
981 breast cancer cells in athymic mice. *Biochem Biophys Res Commun*
982 422(1):139-145.
983 91. Faure S, *et al.* (2005) Xenopus p21-activated kinase 5 regulates
984 blastomeres' adhesive properties during convergent extension
985 movements. *Dev Biol* 277(2):472-492.
986 92. Gong W, *et al.* (2009) P21-activated kinase 5 is overexpressed during
987 colorectal cancer progression and regulates colorectal carcinoma cell
988 adhesion and migration. *Int J Cancer* 125(3):548-555.
989 93. Iioka H, Ueno N, & Kinoshita N (2004) Essential role of MARCKS in cortical
990 actin dynamics during gastrulation movements. *J Cell Biol* 164(2):169-
991 174.
992 94. Rombouts K, *et al.* (2013) Myristoylated Alanine-Rich protein Kinase C
993 Substrate (MARCKS) expression modulates the metastatic phenotype in
994 human and murine colon carcinoma in vitro and in vivo. *Cancer Lett*
995 333(2):244-252.
996

997
998